SECRET

WT-615

Copy No. 254 A

Operation IVY

PACIFIC PROVING GROUNDS

November 1952

Project 5.4a

NATURE, INTENSITY, AND DISTRIBUTION OF FALL-OUT FROM MIKE SHOT

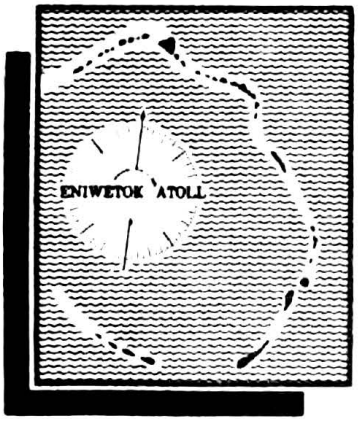

RESTRICTED DATA

This document contains restricted data as defined in the Atomic Energy Act of 1946. Its transmittal or the disclosure of its contents in any manner to an unauthorized person is prohibited.

JOINT TASK FORCE 132

SECRET
SECURITY INFORMATION

SECRET

WT-615

This document consists of 84 pages
No. 254 of 265 copies, Series A

Report to the Scientific Director

NATURE, INTENSITY, AND DISTRIBUTION OF FALL-OUT FROM MIKE SHOT

By

W. B. Heidt, Jr., LCDR, USN
E. A. Schuert
W. W. Perkins
R. L. Stetson

U. S. Naval Radiological Defense Laboratory
San Francisco, California
April 1953

RESTRICTED DATA

SECRET
SECURITY INFORMATION

CHAPTER 1

INTRODUCTION

The gamma-radiation hazard associated with radioactive debris from nuclear explosions constitutes an important capability of atomic weapons. The degree to which this capability can be exploited depends upon the magnitude of the militarily significant gamma-radiation fields produced and upon the ability to predict the location and extent of these fields. The phenomenon, commonly referred to as fall-out, varies with weapon yield and conditions of detonation. The present work proposes to extend the knowledge of such variations by investigating the fall-out material from Mike shot, Operation Ivy. The information derived will be useful for both offensive and defensive planning.

1.1 PREVIOUS FALL-OUT STUDIES

Fall-out from surface and subsurface nuclear detonations has been documented at previous test programs. The phenomenon was first observed after the detonation of the Alamogordo device in 1945.[1] Since that time it has become well established that the gamma hazard resulting from fall-out must be seriously considered as a problem of military significance for all types of detonations except the air burst.* Fall-out was first fully documented at Operation Jangle, but limited data were obtained at Operations Crossroads and Greenhouse.

1.1.1 At Operation Greenhouse

The fall-out study conducted at Operation Greenhouse revealed significant residual contamination from the Dog and Easy tower shots. This investigation was the first comprehensive study of fall-out forecasting.[2] These forecasting techniques, together with the work of J. O. Hirschfelder,[3] are the basis for the theories presented in the discussion of the fall-out at Operation Ivy.

1.1.2 At Operation Jangle

The surface shot at Operation Jangle more nearly represented a miniature Mike shot than any previous detonation. Fall-out studies were made at this operation, and complete data were obtained to a distance of several miles from ground zero.[4] The results were used in planning for Operation Ivy, and certain data to be found herein were extrapolated from information gained from the fall-out studies of Operation Jangle.

---

*An air burst is defined for the purposes of this report as an explosion detonated at an elevation of such height that the resulting fireball at no time touches the surface of the earth.

1.2 OBJECTIVES

The gathering of fall-out data from Mike shot was a logical extension of previous fall-out documentation. The nature of Mike shot, Operation Ivy, made the study of fall-out extremely important. The yield from this shot was expected to exceed by many times that from any previous detonation, and consequently the cloud and associated debris were expected to rise to much greater heights. The additional fact that the shot was to be a surface explosion indicated the possibility of serious fall-out over large areas.

The present work (Project 5.4a) was designed to accomplish the following specific objectives:*

1. To measure the amount, distribution, and particle size of radioactive fall-out following Mike shot at Operation Ivy.
2. To determine at a limited number of close stations the rate of arrival of inert liquid or solid materials and associated radioactive materials.
3. To determine the particle-size fractionation of the radioactive fall-out with time and distance.
4. To analyze the base surge, if formed, for activity and to correlate this information with the fall-out data.
5. To correlate the fall-out pattern obtained with that predicted from a knowledge of the meteorological conditions and atomic cloud behavior.
6. To calculate from the intensities of radiation from fall-out the radiation field levels which would have been observed if the fall-out had occurred over extended land areas.

REFERENCES

1. Los Alamos Scientific Laboratory, "The Effects of Atomic Weapons," pp. 270-275, U. S. Government Printing Office, Washington, 1950.
2. Charles E. Adams, Fall-out Phenomenology, Greenhouse Report, Annex 6.4, WT-4, August 1951.
3. Los Alamos Scientific Laboratory, "The Effects of Atomic Weapons," Appendix F, U. S. Government Printing Office, Washington, 1950.
4. I. G. Poppoff, Fall-out Particle Studies, Jangle Project 2.5a-2 Report, WT-395; also in Particle Studies, WT-371.

*Full attainment of the objectives of this project was not possible because of operational restrictions imposed at a late date. See Appendix D, Tab A (revised) to Appendix I to Annex V.

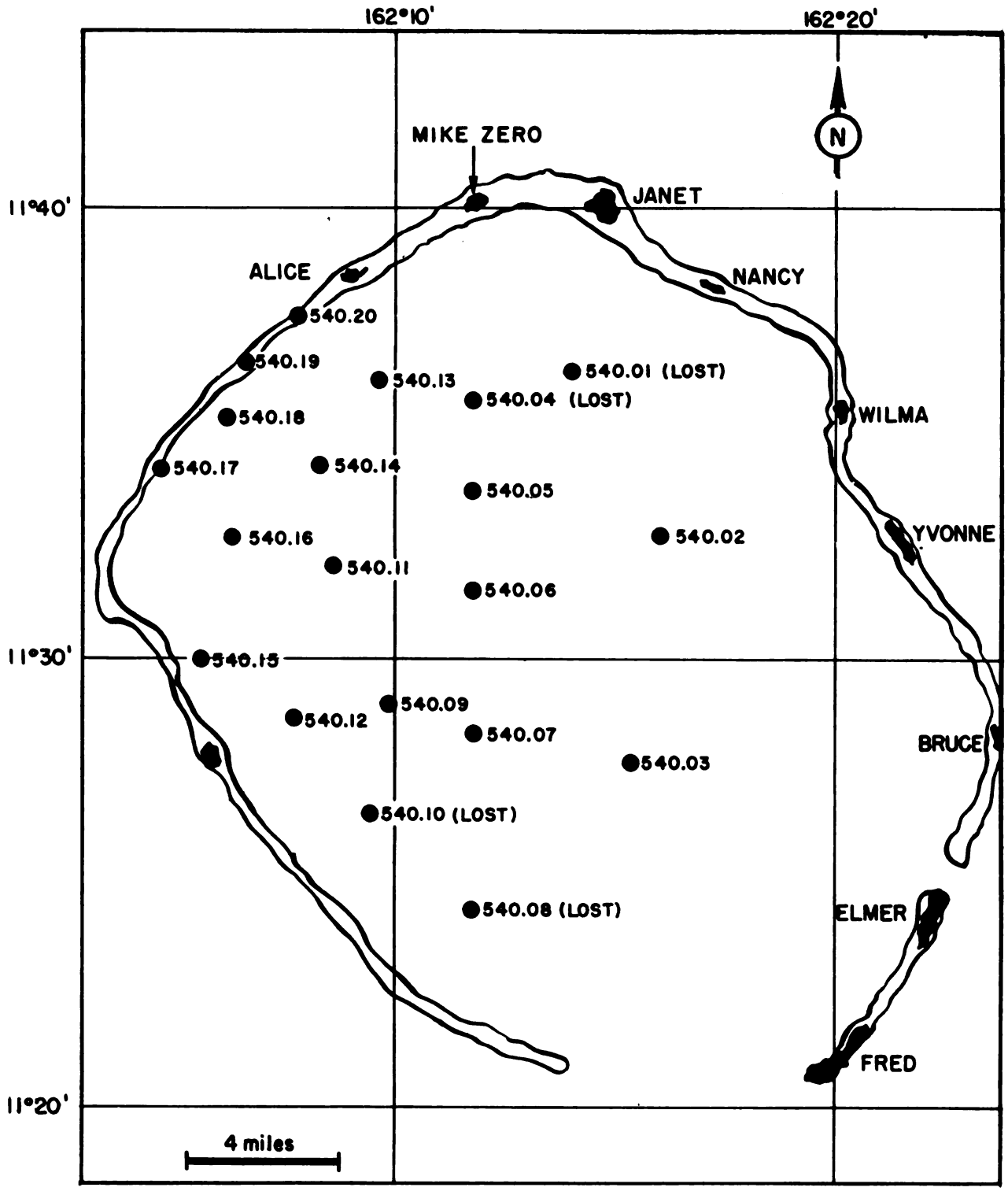

Fig. 2.1—Eniwetok Atoll stations.

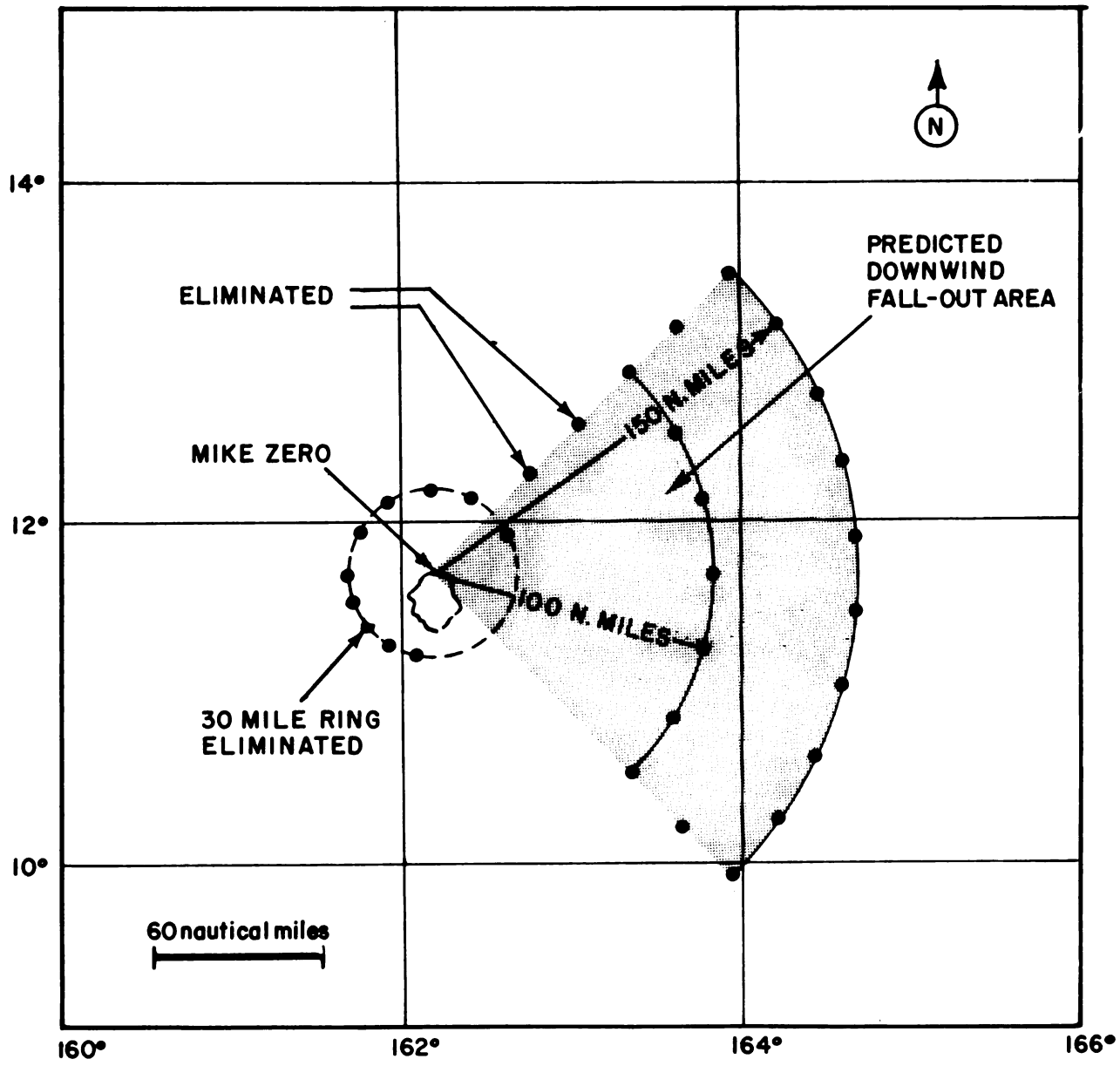

Fig. 2.3—Free-floating sea-station array.

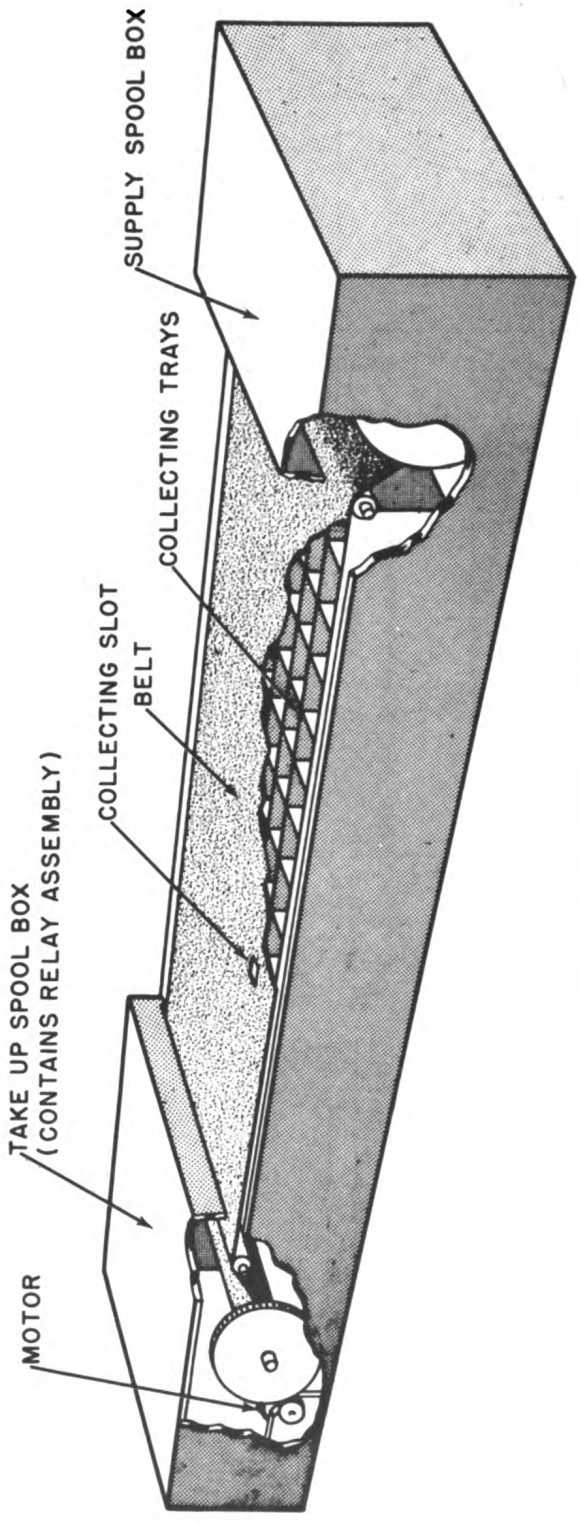

Fig. 3.2—Differential fall-out collector.

3.10.5 Total Collector

This collector gave no trouble except that some fall-out adhered to the collecting funnel.

3.10.6 Ion-exchange Collector

This collector was also trouble free, but, since work is still in progress on the effluent from these columns, no attempt to evaluate them is made.

3.10.7 Gum-paper Collectors

No difficulty was experienced in using these collectors. An excellent feature of the Kum-Kleen adhesive was that, upon exposure, the surface tended to become more tacky rather than drying.

3.10.8 Résumé of the Operation of the Instruments

Table 3.1 shows the disposition and performance of the instruments used at the land and lagoon stations at Eniwetok Atoll.

Table 3.1 — INSTRUMENTATION AT LAND AND LAGOON STATIONS AT ENIWETOK ATOLL

Station	Distance, ft	Total collector	Rain gage	Incremental collector	Differential collector	Trigger	Life float	Remarks
540.20	26,400			Funnel blown off			Moved on-to reef	
540.13	27,050	OK	OK	1½ columns blown off	Belt pulled through	OK	Burned slightly	
540.04	26,400							Lost before shot
540.01	26,400							Lost before shot
540.19	33,000			OK			Moved on-to reef	
540.14	39,600	OK	OK	OK	Belt jammed	OK	OK	
540.05	39,600	OK	OK	OK	Belt tore	OK	OK	
540.18	44,880	OK	OK	Valve open	OK	OK	OK	
540.17	47,520			OK			Moved on-to reef	
540.02	52,800	OK	OK	OK	Belt stuck	OK	OK	
540.11	52,800	OK	OK	OK	Relay failed	OK	OK	
540.06	52,800	OK	OK	OK	Belt stuck	OK	OK	
540.16	55,440	OK	OK	OK	OK	OK	OK	
540.09	68,640	OK	OK	OK	OK	OK	OK	
540.07	71,280	OK	OK	OK	OK	OK	OK	
540.15	72,000	OK	OK	OK	OK	OK	OK	Recovered off reef
540.12	73,920	OK	OK	OK	Belt stuck	OK	OK	
540.03	79,200							Lost
540.10	84,480							Lost before shot
540.08	95,040							Lost before shot
Alice	17,440							Equip. demolished
Janet	18,880	Broken	Broken	Broken	Belt stuck	OK		Equip. demolished
Nancy	33,800	OK	Damaged	OK	OK	Did not trigger		
Wilma	57,180	OK	OK	OK	Belt tore	OK		
Yvonne	75,520	OK	OK	OK	OK	Did not trigger		
Bruce	102,670	OK	OK	OK	OK	Did not trigger		
Elmer	115,060	OK	OK	OK	OK	OK		
Fred	124,580	OK	OK	OK	OK	Did not trigger		

CHAPTER 4

PRIMARY FALL-OUT

Primary fall-out following a nuclear detonation may be defined as the particulate which arrives at relatively early times and forms a well-delineated pattern downwind from ground zero. This fall-out has considerable military significance. The areas of primary fall-out, particularly from superweapons, are quite extensive, and many hours can elapse before the fall-out gamma field is completely defined.

4.1 GAMMA FIELD

The gamma field following Mike shot was well documented within the lagoon. An analysis of the wind profile at shot time indicated that the downwind fall-out lay over the open sea in a swath west-northwest to north of the island where the shot occurred. The data collected at Eniwetok on the Atoll islands and within the lagoon represent primarily the cross-wind pattern and a portion of the upwind region.

Observed Gamma Field. Comprehensive data on the gamma field were obtained within the bounds of Eniwetok Atoll and represent the cross-wind and upwind field. Figure 4.1, showing the gamma field, was compiled from island gamma-survey measurements and lagoon-station gamma-background readings corrected to values representative of the field that would be experienced on an extensive land mass. The gamma values indicated for the lagoon stations are the observed readings multiplied by 7. This multiplying factor results from the relation obtained at Operation Jangle between field gamma readings and gamma measurements of the fall-out from this field as read in a region having a gamma-free background.*[1] Cessation of cross-wind fall-out was at approximately M+2 hr. The field reaches its maximum intensity† at about this time. Figure 4.1 represents the field at M+2 hr. Extrapolation of gamma intensity to M+2 hr was based on the ($t^{-1.2}$) decay law.

No activity was detected from gamma-survey measurements taken over the open water in the lagoon. An examination, primarily of the density of fall-out particulate, indicates that the particulate fell rapidly into the lagoon, where it settled on the bottom and left a zero field at the surface. There was some evidence that the lagoon currents carried a small amount of activity southward from the crater; this was measured by actual water sampling, but the activity had such low intensity that it did not generate a gamma field at the surface.

---

*It is to be understood that the extension of Jangle relations to the soil and water conditions existing at Eniwetok is open to question. The data presented for the lagoon stations in Fig. 4.1 are simply the best approximations.

†As indicated on the Project 5.3 fall-out gamma time-intensity records.

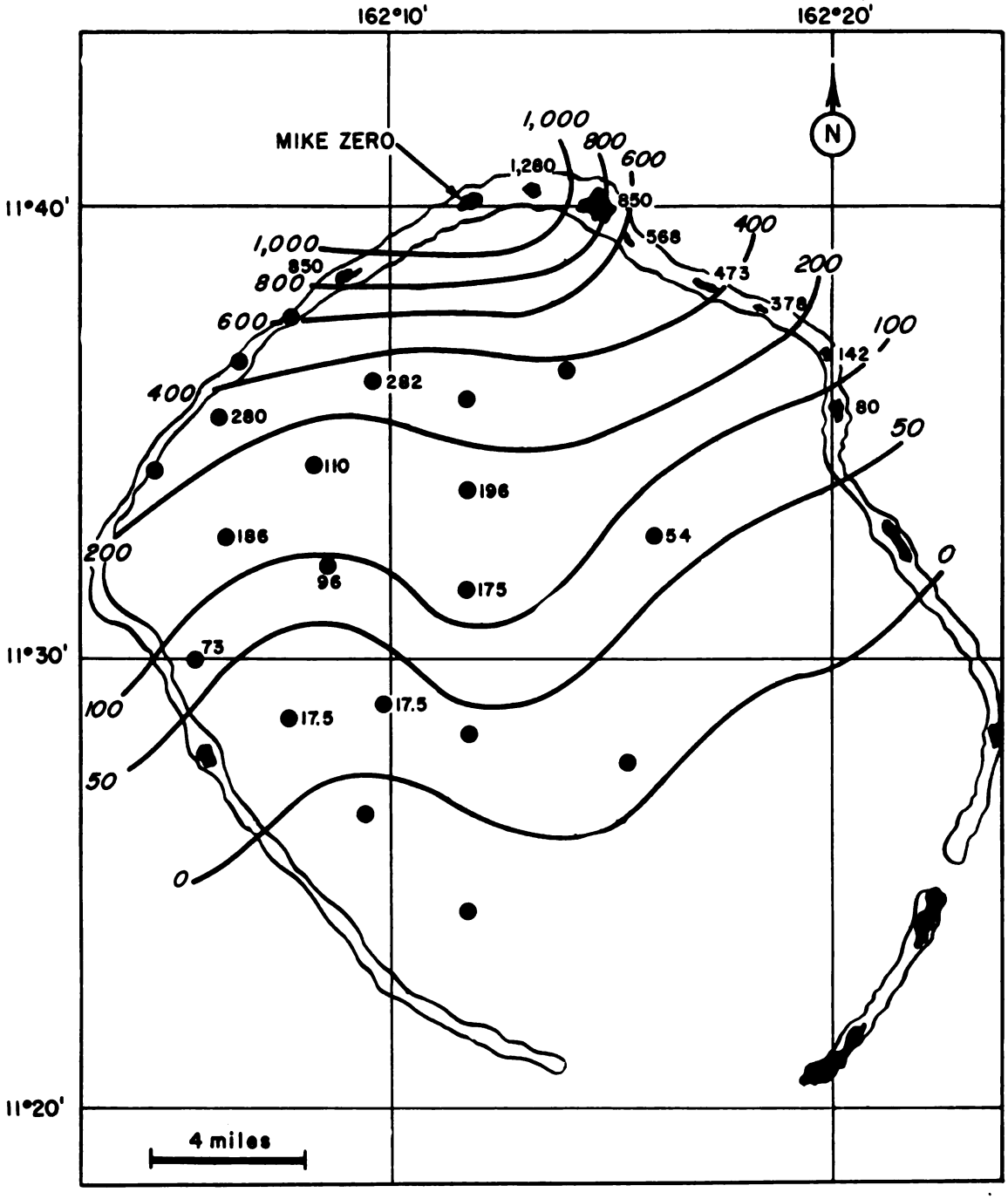

Fig. 4.1—Fall-out gamma pattern at 2 hr as would be experienced on a land mass (r/hr).

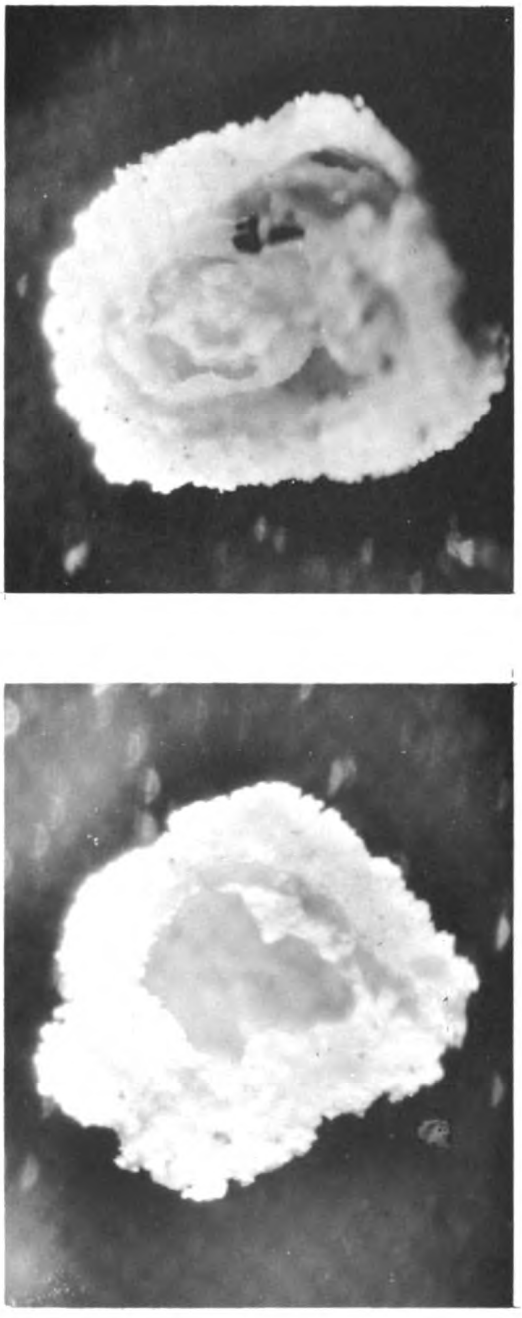

Fig. 4.4—Inverted view of typical particles removed from life-float decking.

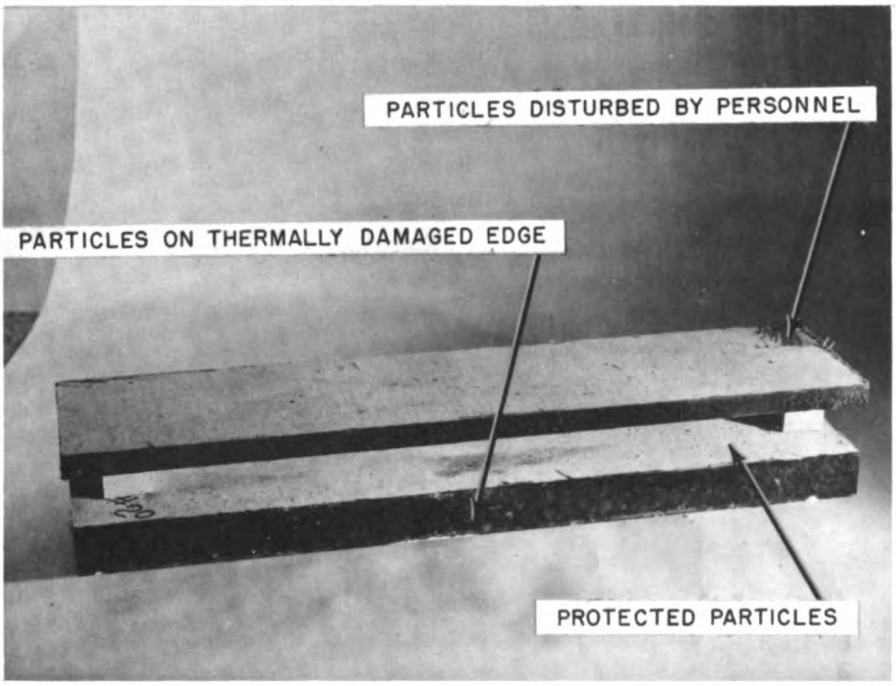

Fig. 4.5—Typical life-float section.

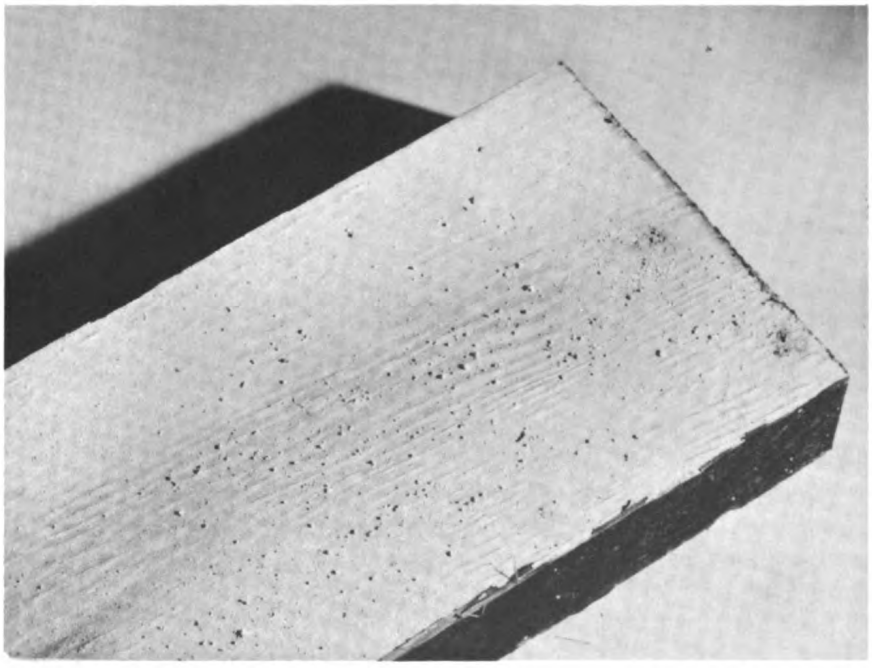

Fig. 4.6—Particle deposition on life-float decking (lower deck of Fig. 4.5).

Table 4.1—SPECTROGRAPHIC ANALYSIS OF THE RADIOACTIVE PARTICLES REMOVED FROM THE LIFE-FLOAT DECKING

Element	Strength of lines*
Al	M
Ba	T
Ca	VS
Fe	T
Mg	VS
Mn	T
Na	M
Si	W
Sr	S
Zn	W

*T = 0.001 to 0.01%.
W = 0.01 to 0.1%.
M = 0.1 to 1%.
S = 1 to 10%.
VS = ≥10%.

Those particles that were deposited on the life-float decking were influenced by a sea-water environment in which there is a comparatively high concentration of magnesium ion, sulfate ion, and a somewhat smaller one of bicarbonate ion. As the sea water slowly dissolved the slightly soluble calcium hydroxide in the particles, the liberated hydroxide ions reacted with the magnesium ions in the sea water to form a shell of insoluble magnesium hydroxide around the particles. On the exterior of the magnesium hydroxide shell, a layer of calcium carbonate was formed from the dissolved calcium ions and the bicarbonate ions of the sea water. On the interior of the shell, calcium ions from the soluble calcium hydroxide were precipitated by the sulfate ions of the sea water to form a zone of well-developed hydrated calcium sulfate crystals (gypsum).

The prolonging of this leaching and precipitation process caused the formation of either completely or partially hollow particles.

The radioactivity was found to be associated primarily with the inner core of undissolved calcium hydroxide. Little or no activity was found in the magnesium hydroxide–calcium carbonate shell or in the calcium sulfate crystals.

This leaching, by causing a partial solution and reprecipitation of the soluble calcium compounds, accounts for the adherence of the particles to the life-float decking.

4.2.3 Leaching of Activity

The total collectors, consisting of a funnel and bottle, were exposed several days before the shot and were not collected until several days thereafter. Consequently there was a considerable amount of rain water in each collector, as well as a sample of the total fall-out. It was found that the liquid portion collected was active, and analysis of the samples showed that from 14 to 80 per cent of the total activity in the collectors was in the solid particulate. The average amount of leaching of activity into the rain water was approximately 50 per cent. No correlation could be found between location of the collector and the amount of leaching.

Approximately 0.1 g of particulate that was collected in the dry state was allowed to leach in a surplus (500 cu cm) of distilled water for over one week to see whether there was a cor-

relation between the ratio of activities and the ratio of mass before and after leaching. The ratio of the weight of solid remaining after leaching to the original weight was 48 per cent, whereas the ratio of the activity in the leached solid to the total activity of the solid before leaching was 54 per cent.

Table 4.2—X-RAY-DIFFRACTION ANALYSIS OF RADIOACTIVE PARTICLES REMOVED FROM THE DIFFERENTIAL FALL-OUT COLLECTORS

Station	Compounds present	Compounds probably present	Remarks
Janet	$CaCO_3$ (calcite) $CaCO_3$ (artificial calcite) $Ca(OH)_2$ (Portlandite) $CaCO_3$ (aragonite)		
Wilma		$CaCO_3$ (aragonite)	Amount of sample less than 1 mg; identity of compound not certain
540.16	$CaCO_3$ (calcite) $CaCO_3$ (artificial calcite)	Unknown compounds of large lattice spacings	See Station 540.18 remarks
540.18	$CaCO_3$ (calcite) $CaCO_3$ (artificial calcite) $Ca(OH)_2$ (Portlandite) $CaCO_3$ (aragonite) NaCl (halite)	Unknown compounds of large lattice spacings	The unknown compounds of large lattice spacings are not all the same; preliminary determinations have shown them to be the less common compounds; further research is needed to determine their nature
540.13	$Ca(OH)_2$ (Portlandite) $CaCO_3$ (calcite) NaCl (halite) $CaCO_3$ (artificial calcite)		
540.14	$CaCO_3$ (calcite) $CaCO_3$ (artificial calcite) MgO (periclase)	Unknown compounds of large lattice spacings	See Station 540.18 remarks
540.09		$CaCO_3$ (aragonite)	Amount of sample less than 1 mg; identity of compound not certain

The liquid from the total collector located at Station 540.18 was analyzed to determine the percentage of activity from ions and that from colloids. This analysis was done by ultrafiltration at 38 atm through a cellophane dialyzing membrane with a pore size in the range of 12 to 40 A. It was found that 71 ± 3 per cent of the activity was associated with the ionic species and 29 ± 4 per cent with the colloids. Since this liquid sample had been previously filtered through Whatman No. 30 paper, some of the colloids remained with the particulate caught by the filter.

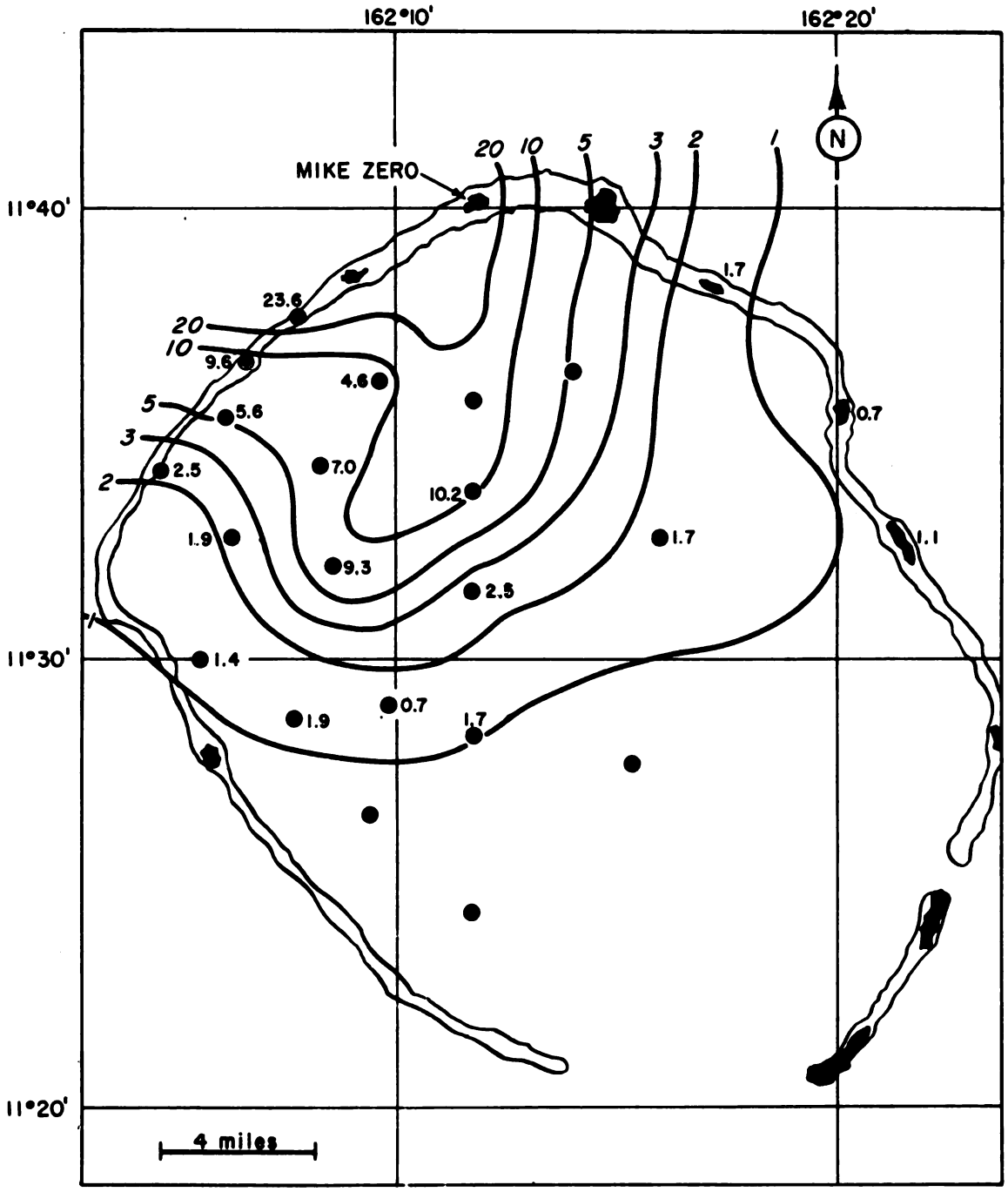

Fig. 4.8—Mass distribution of fall-out (g/sq ft).

shown in Fig. 4.11. Stations 540.15 and 540.09 were both located at 15 miles, but at different azimuths from ground zero (see Fig. 2.1 for location).

4.5.1 Arrival of Fall-out

It is most interesting to note that the cross-wind arrival time was completely independent of distance from ground zero. At the four stations from 8 to 15 miles, the fall-out began at +40 to +45 min. This suggests a delivery mechanism independent of winds (Chap. 6).

Table 4.3—SIZE DISTRIBUTION OF RADIOACTIVE FALL-OUT PARTICLES

Station	Distance cross wind, miles	Period of fall-out	Size distribution, μ: 25 to 50	50 to 100	100 to 200	200 to 300	300 to 400	Remarks
540.20	5.0	Early	4	8	14	5	7	Several particles to 5000 μ
540.18	8.0	Early	6	10	2			Several particles to 1200 μ
540.18	8.0	Middle	1	4	7	4	1	Several particles to 500 μ
540.17	10.0	Middle	1	2	10	1		Several particles to 1000 μ
540.16	10.0	Early	9	23	1	3		
540.15	15.0	Middle	0	2	1			Several particles to 1200 μ
540.15	15.0	Late	13	13	12	3		Several particles to 1200 μ

4.5.2 Duration of Fall-out

The four stations fixed the duration of fall-out at something less than 2 hr, with three of these stations experiencing exactly the same duration. Station 540.09, to the east of 540.15, shows the cessation of the fall-out to be at 0 + 95 min, a somewhat earlier time than the time of 0 + 144 min experienced by the other three stations.

4.5.3 Distribution of Activity with Time

Figure 4.11 shows the randomness of the time distribution of fall-out within the period in which it occurred. All the stations experienced several maxima and minima. These peaks and valleys show no correlation between time and distance. Since the samples were collected over limited areas, the levels of activity shown in Fig. 4.11 are not too representative.

REFERENCES

1. I. G. Poppoff, Fall-out Particle Studies, Jangle Project 2.5a-2 Report, WT-395; also in Particle Studies, WT-371.
2. U. S. Naval Radiological Defense Laboratory Report on High Explosive Model Studies (in preparation).

CHAPTER 6

METEOROLOGICAL CONSIDERATIONS AND FORECASTS OF FALL-OUT

Knowledge of the mechanism of the fall-out phenomenon is necessary as a first step in the development of forecasting techniques that will satisfactorily define the gamma field created by the residual radioactive debris from a nuclear detonation. Fall-out gamma fields of military significance are known to develop with surface and underground or underwater nuclear explosions, and the problem of fixing both the location and extent of the resultant radiation field is paramount for either offensive or defensive operations. Solution of this problem requires knowledge of the shot location, an estimate of the resulting cloud height, and the wind speed and direction to an elevation equal to the height of the explosion cloud.

6.1 THEORIES OF FALL-OUT MECHANISM

J. O. Hirschfelder's analysis[1] satisfactorily explains the mechanism of fall-out, except for the area immediately surrounding ground zero at Operation Ivy.

The theory developed by Charles E. Adams[2] accounts for the phenomenology of the fall-out in the area in the immediate vicinity of ground zero.

It is believed that these theories in their respective areas accounted for the fall-out phenomena accurately at Operation Ivy.

6.2 PRIMARY FALL-OUT

No data were collected downwind from ground zero. Figure 6.1 represents the downwind fall-out area as defined by the Hirschfelder analysis.

The cross-wind data showing the arrival time to be independent of distance can be satisfactorily explained by the vertical-circulation theory as explained by Adams in the Greenhouse fall-out studies. If a cloud chimney 5 miles in diameter is assumed to contain rising air currents, there is reason to believe descending currents exist around this upward convection column out to a distance equal to several column diameters. This vertical circulation is analogous to the circulation around a thunderstorm. A subsidence of this type would deposit particulate of heterogeneous mixture out to approximately 15 miles, and the time of deposition would be independent of distance.

Therefore the primary fall-out pattern is believed to have developed by two separate and distinct mechanisms: first, a subsidence extending out to several cloud diameters and, second, a downwind pattern determined by particle settling rates and the wind profile. This downwind pattern is based on the assumption that the particulate source is the cloud chimney from the

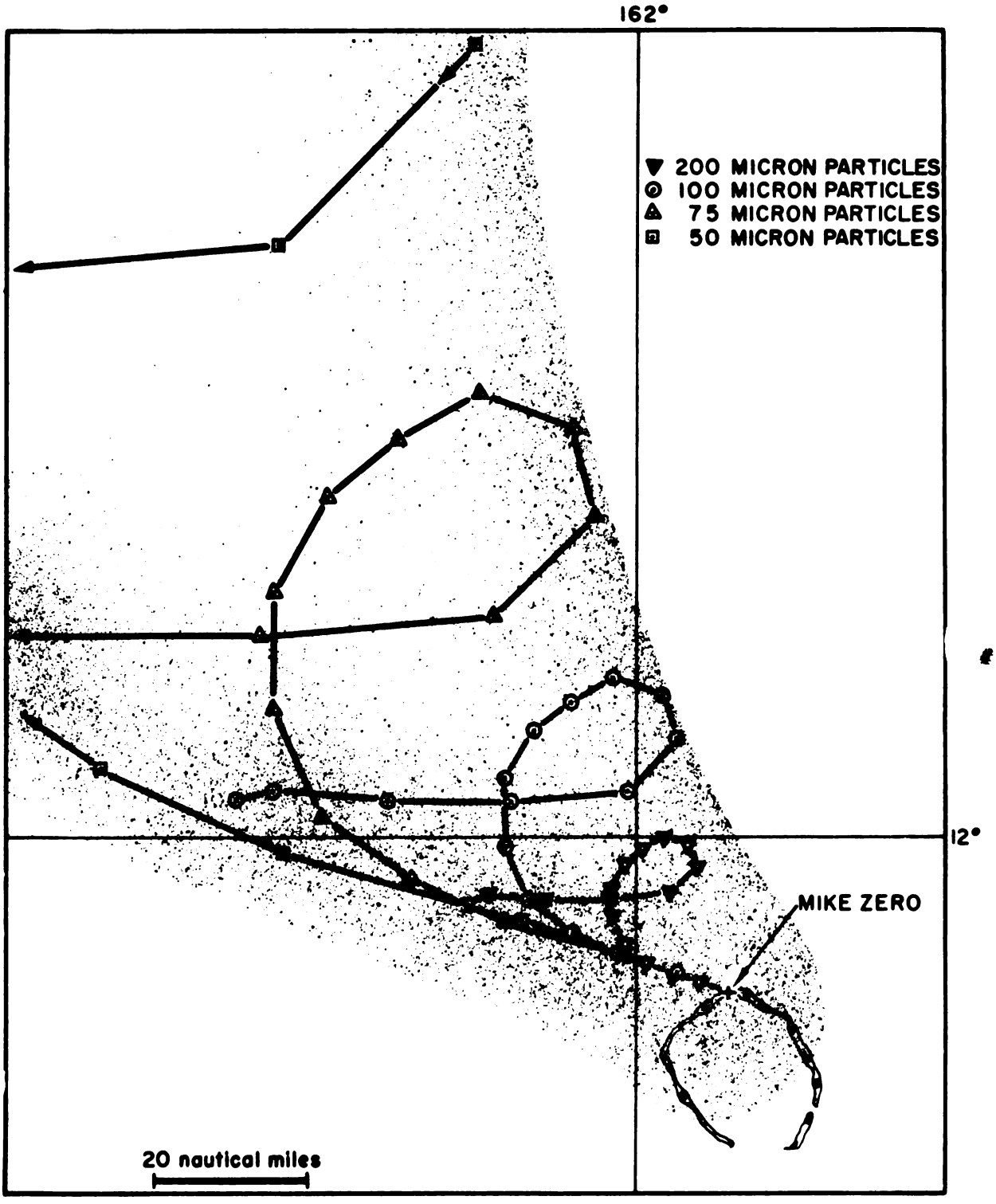

Fig. 6.1—Predicted area of primary fall-out.

surface to the cloud's maximum elevation, with a heterogeneous particle-size mixture existing throughout. The points of arrival of particle sizes from all elevations define the downwind pattern with respect to both area and time of arrival.

6.3 SECONDARY FALL-OUT

The winds in the Marshall Islands area above 90,000 ft are predominantly from the west at the time of the year of Operation Ivy.[3] The cloud from Mike shot rose to a height greater than 100,000 ft and was observed to move to the east. The few winds above 90,000 ft observed during the operation by the task force Weather Central were from the west.

The arrival time of the secondary fall-out can be satisfactorily explained by assuming that the particulate originated in the uppermost portion of the cloud, carried eastward by the stratospheric winds. Since the particulate settled into the troposphere somewhere east of the Marshall Islands area, an examination of the troposphere wind pattern during the days following the detonation showed that the particulate would be carried back westward and deposited as secondary fall-out in the area investigated.

6.4 THE EFFECT OF VERTICAL MIXING

The arrival time of small particulate at distances beyond the area of subsidence has defied explanation by particle settling rates. This failure is especially evident when considering arrival times of secondary fall-out. It is suggested that for particles whose diameter and density establish slow settling rates the effect of vertical mixing in the atmosphere becomes the primary mechanism determining their deposition.

REFERENCES

1. Los Alamos Scientific Laboratory, "The Effects of Atomic Weapons," Appendix F, U. S. Government Printing Office, Washington, 1950.
2. Charles E. Adams, Fall-out Phenomenology, Greenhouse Report, Annex 6.4, WT-4, August 1951.
3. C. E. Palmer, The Central Pacific Project, First Report, Institute of Geophysics, October 1951.

CHAPTER 7

SUMMARY

Prediction of the downwind area of primary fall-out with a high degree of confidence early enough to establish a selective station array to cover the area cannot be satisfactorily accomplished. The limited climatological data available for the Marshall Islands indicate the most probable direction of the winds aloft during the fall and winter months to be from the east for heights of approximately 20,000 ft and from the west for heights between 20,000 and 100,000 ft. However, the wind profile at shot time indicated that the primary fall-out following Mike shot was deposited to the northwest of Eniwetok Atoll. It is noteworthy that during the two weeks prior to shot time, the daily variation in the wind profile was of such magnitude that a 24-hr forecast of the fall-out area would have been in error in the majority of cases. However, if the winds aloft are known at the time of detonation, it is possible to predict quite accurately the distribution of ground contamination resulting from radioactive fall-out.

Observation of the documentary photography taken of Mike shot, Operation Ivy, indicated no evidence of a base surge following the detonation. Although the major portion of this film did not record surface phenomena, those portions documenting the surface of the lagoon after the event do not show a base surge.

The fall-out particulate, being primarily compounds of calcium, was peculiar to a coral atoll. The main contribution to the radiation field was the fission product mixture trapped within these particulates. The particle density was between 1 and 3 g/cu cm in the majority of cases and similar to that of many soils. Although there was not a great quantity of fall-out at any location, the individual particles were very active, some reading as high as 300 mr/hr of beta-gamma radiation 48 hr after shot time. The activity was easily leached from the particulate by the action of rain water. The particle reaction with the sulfate ions in sea water caused them to become hollow and to adhere to any surface they touched. This behavior is probably the most significant observation of the effect of the environment on the particles.

7.1 CONCLUSIONS

In summarizing the work done on this project, it is convenient to state the conclusions as they specifically apply to either the primary or secondary fall-out.

7.1.1 Primary Fall-out

The gamma-radiation field at the cessation of the primary fall-out varied from about 800 r/hr at 2 hr and 3 miles distance to 0 r/hr at a cross-wind distance of approximately 15 miles.

There was no residual radiation field over the open water of the lagoon. Evidently the radioactive particulate immediately settled to the bottom.

The gamma decay curve for the radioactive fall-out has a slope of approximately -1.2.

The fall-out was solid particulate made up of calcium hydroxide with a very thin layer of calcium carbonate on the outer surface. The fission products were trapped within the particulate.

Those particles that arrived in such an environment as sea-washed decking were slowly dissolved, with a resulting reprecipitation of the calcium ion by the sulfate ion which exists in comparatively high concentration in sea water. As a result of this phenomenon, many hollow particles formed and firmly adhered to all surfaces they touched.

The fission products readily leached from the particulate exposed to rain water. The leached activity was both ionic species and colloids.

The quantity of primary fall-out in the cross-wind direction varied from some value over 20 g/sq ft at 4 miles to 0 g/sq ft at 15 miles.

The particle diameters of the radioactive fall-out varied from less than 10 μ to greater than 5000 μ.

There was no particle-size fractionation with cross-wind distance and only meager evidence of any with time.

The cross-wind fall-out arrival time was entirely independent of distance from ground zero; duration of fall-out was approximately 1 to 2 hr.

There was a random distribution of activity with time at all stations in the cross-wind radiation field.

7.1.2 Secondary Fall-out

Secondary fall-out arrived over an extensive area of the Pacific around Eniwetok Atoll.

The period of secondary fall-out was several days at any one location, arriving from 2 to 5 days after the detonation.

None of the secondary fall-out was of military significance since a gamma dose rate of less than 10 mr/hr was noted at all collecting stations.

In no case was any of the secondary fall-out particulate over 25 μ in diameter.

The secondary fall-out arrived from an initial height greater than 80,000 ft.

7.2 RECOMMENDATIONS

Experience gained during the work on this project makes possible certain suggestions for consideration in the planning of future operations. The inability to predict the area of primary fall-out well in advance of shot time can be presumed to be definitely established. Consequently it is recommended that a 360° coverage of collecting stations be provided in future tests.

Furthermore the use of free-floating stations can be considered practical and highly desirable if a method for their positive location is provided. Whatever methods that are devised for locating the free-floating stations must not interfere with the task force security search patrol. Therefore it is recommended that a lightweight coded signaling device such as the British Ultra Air Sea Rescue beacon be installed on each of the free-floating stations.

WT-915

Copy No. [illegible]8

Operation
CASTLE

PACIFIC PROVING GROUNDS

Project 2.5a

DISTRIBUTION AND INTENSITY OF FALLOUT

[redacted]

[redacted]

Sec 131 - AEC

HEADQUARTERS FIELD COMMAND, ARMED FORCES SPECIAL WEAPONS PROJECT
SANDIA BASE, ALBUQUERQUE, NEW MEXICO

WT-915

This document consists of 172 pages

No. 238 of 240 copies, Series A

OPERATION CASTLE

Project 2.5a

DISTRIBUTION AND INTENSITY OF FALLOUT

REPORT TO THE SCIENTIFIC DIRECTOR

by

R. L. Steton
E. A. Schuert
W. W. Perkins
T. H. Shirasawa
H. K. Chan

(Misprint: correct spelling of first author is Stetson, not Steton.)

January 1956

[redacted]

U. S. Naval Radiological Defense Laboratory
San Francisco 24, California

[redacted]

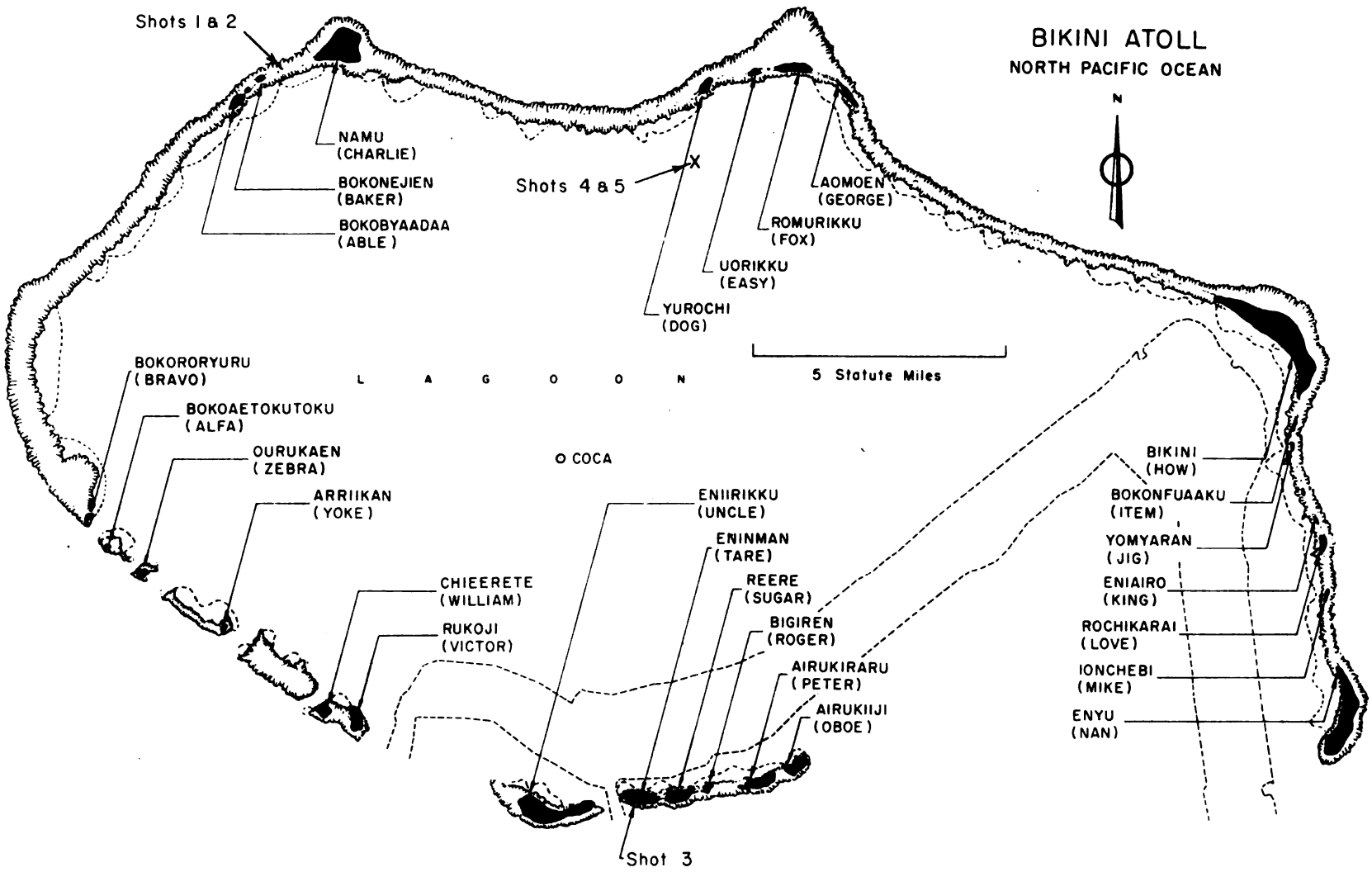
BIKINI ATOLL
NORTH PACIFIC OCEAN
N
Shots 1 & 2
NAMU
(CHARLIE)
BOKONEJIEN
(BAKER)
BOKOBYAADAA
(ABLE)
Shots 4 & 5
X
AOMOEN
(GEORGE)
ROMURIKKU
(FOX)
UORIKKU
(EASY)
YUROCHI
(DOG)
5 Statute Miles
BOKORORYURU
(BRAVO)
L A G O O N
BOKOAETOKUTOKU
(ALFA)
OURUKAEN
(ZEBRA)
O COCA
ARRIIKAN
(YOKE)
ENIIRIKKU
(UNCLE)
ENINMAN
(TARE)
CHIEERETE
(WILLIAM)
REERE
(SUGAR)
RUKOJI
(VICTOR)
BIGIREN
(ROGER)
AIRUKIRARU
(PETER)
AIRUKIIJI
(OBOE)
Shot 3
BIKINI
(HOW)
BOKONFUAAKU
(ITEM)
YOMYARAN
(JIG)
ENIAIRO
(KING)
ROCHIKARAI
(LOVE)
IONCHEBI
(MIKE)
ENYU
(NAN)

GENERAL SHOT INFORMATION

	Shot 1	Shot 2	Shot 3	Shot 4	Shot 5	Shot 6
DATE	1 March	27 March	7 April	26 April	5 May	14 May
CODE NAME (Unclassified)	Bravo	Romeo	Koon	Union	Yankee	Nectar
TIME*	06:40	06:25	06:15	06:05	06:05	06:15
LOCATION	Bikini, West of Charlie (Namu) on Reef	Bikini, Shot 1 Crater	Bikini, Tare (Eninman)	Bikini, on Barge at Intersection of Arcs with Radii of 6900' from Dog (Yurochi) and 3 Statute Miles from Fox (Aomoen).		Eniwetok, IVY Mike Crater, Flora (Elugelab)
TYPE	Land	Barge	Land	Barge	Barge	Barge
HOLMES & NARVER COORDINATES	N 170,617.17 E 76,163.98	N 170,635.05 E 75,950.46	N 100,154.50 E 109,799.00	N 161,698.83 E 116,800.27	N 161,424.43 E 116,688,15	N 147,750.00 E 67,790.00

* APPROXIMATE

ABSTRACT

The objective of this project was to document the distribution and intensity of fallout from all shots at Operation CASTLE.

Data were obtained for Shots 1, 2, 3, 4, and 6 by use of land stations, anchored lagoon stations, and free-floating sea stations. A complete analysis of the Shot 1 fallout to 300 nautical miles downwind including the development of an experimental model based on fallout particle trajectories is presented as well as data on Shot 2 fallout to 50 nautical miles downwind and the close-in fallout from Shots 3, 4, and 6.

Gamma fields from fallout decayed at rates differing from the $t^{-1.2}$ approximation commonly applied to fission weapons.

Fallout from the surface land detonations was in the form of irregular solid particulates. The geometric mean particle diameter decreased with the distance from the shot points; for Shot 1 the geometric mean varied from 112 μ at Bikini Atoll to 45 μ at Utirik Atoll. The average density of the solid particles from Shot 1 was 2.36 g/cu cm. Little data were obtained on the nature of the fallout from over-water detonations. There was some indirect evidence that the fallout 50 nautical miles downwind from Shot 2 arrived as a fine mist or aerosol. The rate of arrival of fallout at distances close to surface zero was characterized by a rapid rise to a peak; the maximum level of radiation occurred within the first half of the period of fallout.

A continuous 100 hr unshielded exposure after the detonation of a 15-MT device on land, will result in a minimum free field total dose of 100 r over an area as large as 25,000 sq mi.

There is developed an experimental model that provides a means of reconstructing fallout patterns from limited gamma field data and particle trajectories as determined by comprehensive analyses of the meteorological situation.

[redacted]

CHAPTER 1

INTRODUCTION

Surface and sub-surface detonations of nuclear weapons on land produce hazardous gamma-radiation fields over areas far beyond the range of physical damage. Fallout which is responsible for the gamma-radiation fields is inherently the least predictable of all weapons effects. Variations in the dispersal and deposition of radioactive debris are affected by meteorological conditions during and subsequent to detonation as well as by the device yield, the charge depth, and the explosion media. Yet, the exploitation of this anti-personnel capability, and the capacity to defend against it, are directly dependent upon the ability to predict those target areas which will be involved. The investigation of fallout, and of the factors which influence it, are therefore important to the development of nuclear weapons and to both military and civil defense planning.

1.1 PREVIOUS FALLOUT STUDIES

Fallout has been observed and documented in some degree at all previous nuclear test programs. In addition, surface and sub-surface high explosive detonations on land and underwater are being studied for their usefulness as models for fallout distribution from nuclear detonations.

1.1.1 Nuclear Tests

Out of a total of 43 nuclear test explosions carried out by the United States, four have produced significant residual radiation fields, the Baker shot, Operation CROSSROADS, surface and underground shots, Operation JANGLE, and Mike shot, Operation IVY. Of these four, only the JANGLE series adequately had documented fallout.

At JANGLE, the residual gamma fields were recorded in detail; in addition, extensive sampling of the fallout events was carried out.[14] Results of the JANGLE surface test were used to predict fallout from Mike shot, IVY. They also formed a basis for fallout predictions for the CASTLE series reported here.

At IVY, although only partial documentation was accomplished,

[redacted]

[redacted]

the operational success of the free-floating buoy station phase was sufficient to encourage the employment of this fallout sampling technique at CASTLE.7/ IVY provided valuable data on the extent of the crosswind and upwind fallout and on the nature of the contaminant to be expected from the land surface detonations at CASTLE.

1.1.2 High Explosive Tests

Six high explosive field tests have been conducted to study fallout. Charges varying from 250 to 50,000 lb of TNT were fired. Emphasis has been placed on shallow underwater explosions.16/ Of a total of 38 shots, 26 were fired in shallow water; 5 in deep water; and 7 on land, both surface and underground. Non-radioactive cobalt and lithium were incorporated in the charges to trace the explosion products. Variables under study include energy yield, charge depth, explosion media, and wind.

1.2 OBJECTIVES

The surface detonations of thermonuclear devices at Operation CASTLE were expected to produce significant fallout over considerable portions of the ocean at the Pacific Proving Ground. The primary purpose of Project 2.5a was to document these fallout areas and determine the militarily important radiation fields which would have resulted had all of the material been deposited on land. Specifically, Project 2.5a was designed to determine the following information for selected shots:

a. Time and rate of fallout and final distribution patterns.
b. Particle size ranges of fallout with respect to time and distance.
c. Amount and distribution of radioactive materials in fallout.
d. Gross gamma decay rates.

The gathering of fallout data at CASTLE was a logical extension of previous fallout documentation. Variation in proposed yields as well as the opportunity to document surface water detonations for the first time made the study of fallout in this operation extremely important.

[redacted]

(FO_L) and the corresponding field radiation intensity, (R_L); (2) determining the fallout per unit area over water, (FO_W) and; (3) calculating the radiation field, (R_W) which would have occurred had the water areas been land, from the assumed relationship,

$$R_W = R_L \frac{FO_W}{FO_L} \qquad (2.1)$$

This method of approach required the following measurements:

(a) Fallout per unit area on available islands of the test atolls in terms of quantity of radioactivity.

(b) Gamma fields produced at sampling locations.

(c) Fallout per unit area in the lagoon and over the surrounding ocean. It was also important to obtain information concerning particle size and note times of arrival and cessation of the fallout as well as the variations in the radiation field with time.

2.1.1 Predicted Gamma Fields

Estimates of the extent and level of gamma fields expected from the fallout were made for each of the originally planned shots. These predictions were based on scaled surface JANGLE data using the cube root relationship with modifications in the crosswind and upwind patterns indicated by IVY data.7/ It was estimated that the fallout would carry downwind at the rate of 15 miles per hour and that the duration of fallout at any one point would be 2 hr for megaton yields. Values calculated for 2 and 3 hr after detonation represent the levels that would exist had the fallout deposited over extended land areas. Table 2.1 summarizes the predictions for three of the detonations; the effect of decay and the delay in arrival of fallout on the gamma fields can be noted. A discussion of this scaling is presented in Section 6.2.8.

2.1.2 Sampling Stations

On the basis of the predictions given in the preceding section, it appeared that the minimum area of military interest would extend to a distance of 50 miles from the shot point and would have a maximum width of 20 miles. Since it was not possible to predict the sector in which the primary fallout would arrive sufficiently in advance of shot time to permit proper placement and activation of sampling stations, an array completely surrounding the shot point was needed. Experience at IVY showed that, it would not be feasible to document the fallout more than 50 miles from ground zero with available logistic support. The radial array of sampling stations shown in Fig. 2.1 was evolved from these criteria. This plan was modified within the atolls to take advantage of available islands and to permit the placement of simple rectangular grid arrays in the lagoons. In addition, limited sampling stations were arranged at a number of outlying islands.

Operationally, Project 2.5a was divided into two phases - one requiring the collection of data from land and lagoon stations, and the other from sea stations. Logistic support for the land and lagoon phase involved the use of small boats and helicopters while mounting of the

TABLE 2.1 - Predicted Downwind Contamination Levels for Shots 1,2, and 5 after Detonation
(r/hr at times indicated)

Shot	5 n mi		10 n mi		15 n mi		20 n mi		25 n mi		30 n mi	
	2 hr	3 hr	2 hr	3 hr	2 hr	3 hr	2 hr	3 hr	2 hr	3 hr	2 hr	3 hr
1 (based on 6 MT yield)	10,000	5000	5000	4000	3000	3000	1200	2000	800	1500	0	800
2 (based on 3 MT yield)	7,000	4000	3000	2500	1300	1500	700	1100	200	400	0	200
5 (based on 8.5 MT yield)	12,000	7000	6000	5000	4000	4000	2000	2000	1000	2000	0	1000

sea phase required employment of sea-going vessels under the Naval Task Group Command.

2.1.2.1 Land Stations

At Bikini, the islands of Able, Fox, How, Love, Nan, Oboe, Uncle, William, Yoke, and Zebra, were used for sampling and obtaining gamma field measurements. Stations consisted of concrete emplacements with instruments installed in and about them.

At Eniwetok, the islands of Irene, Bruce, Yvonne, Wilma, Leroy, Alice, Janet, and Nancy were used for sampling and for obtaining gamma field measurements. Where possible, station emplacements remaining from IVY fallout sampling were utilized; otherwise instruments were placed in the open and suitable tie-down arrangements improvised.

Stations were established on the following outlying islands: Rongerik, Kusaie, Majuro, Ponape, Wake, Guam, Kwajalein, and Johnson.

2.1.2.2 Lagoon Stations

Rectangular-grid arrays of stations were established for lagoons of both test atolls, as shown in Figs. 2.2 and 2.3. These consisted of anchored buoys to which rafts were attached (see Fig. 2.4).

2.1.2.3 Sea Stations

Sampling in the open ocean was accomplished by means of free-floating buoys to which, in some cases, rafts were attached. Plans were made to provide the complete coverage indicated by Fig. 2.1 for one land

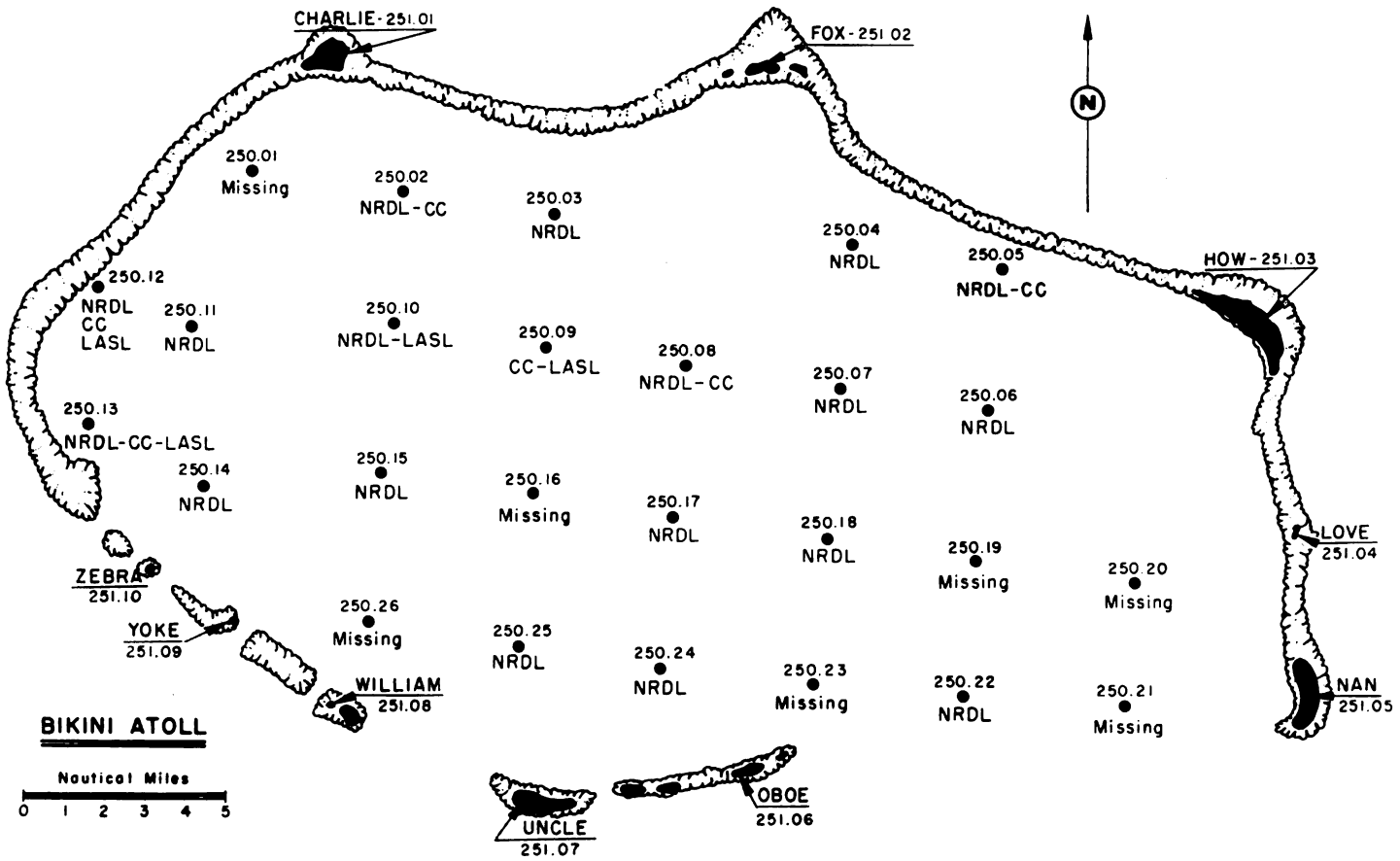

Fig. 2.2 Lagoon and Island Station Array for Bikini Atoll

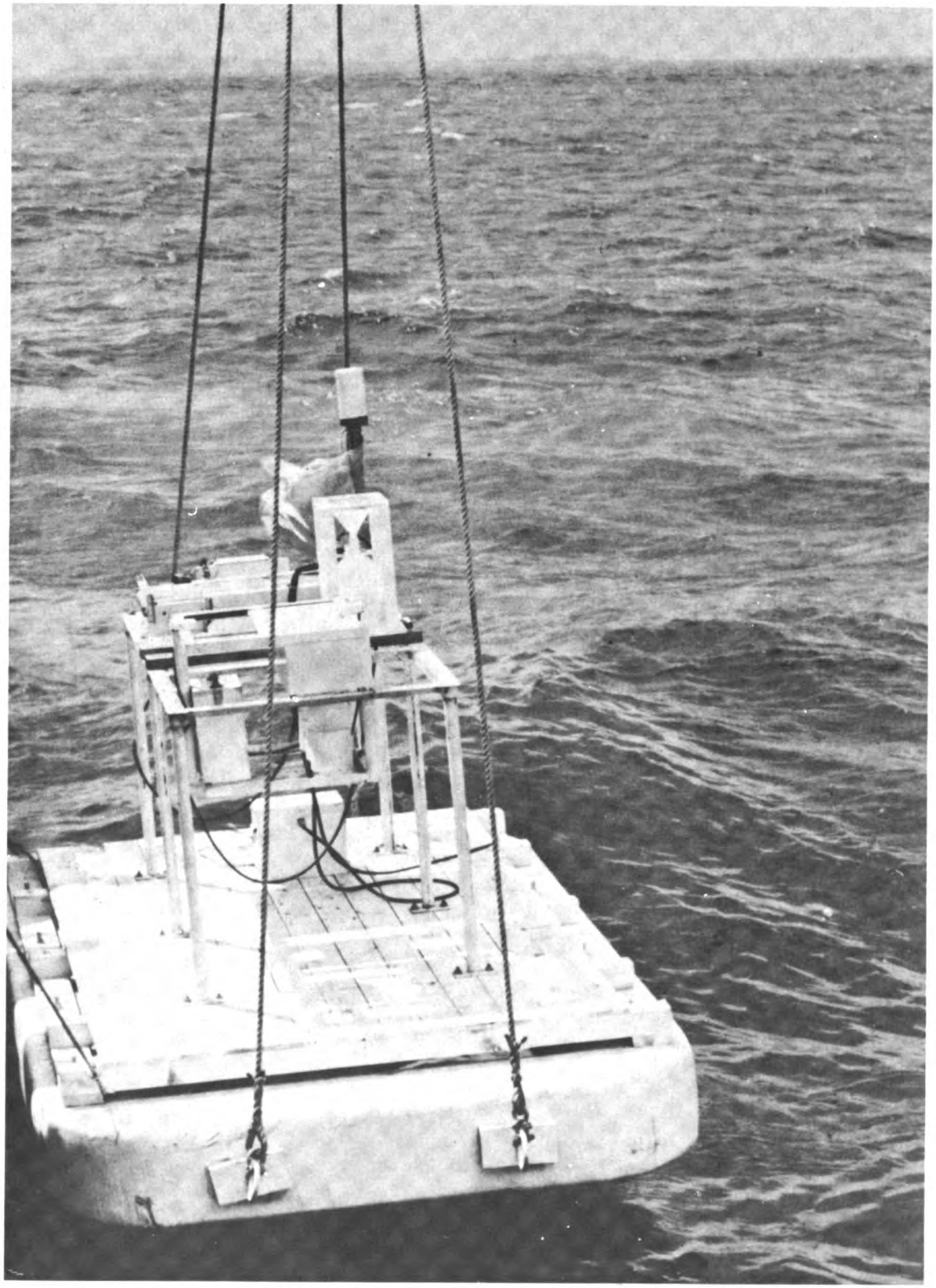

Fig. 2.4 Lagoon Station Being Placed

[redacted]

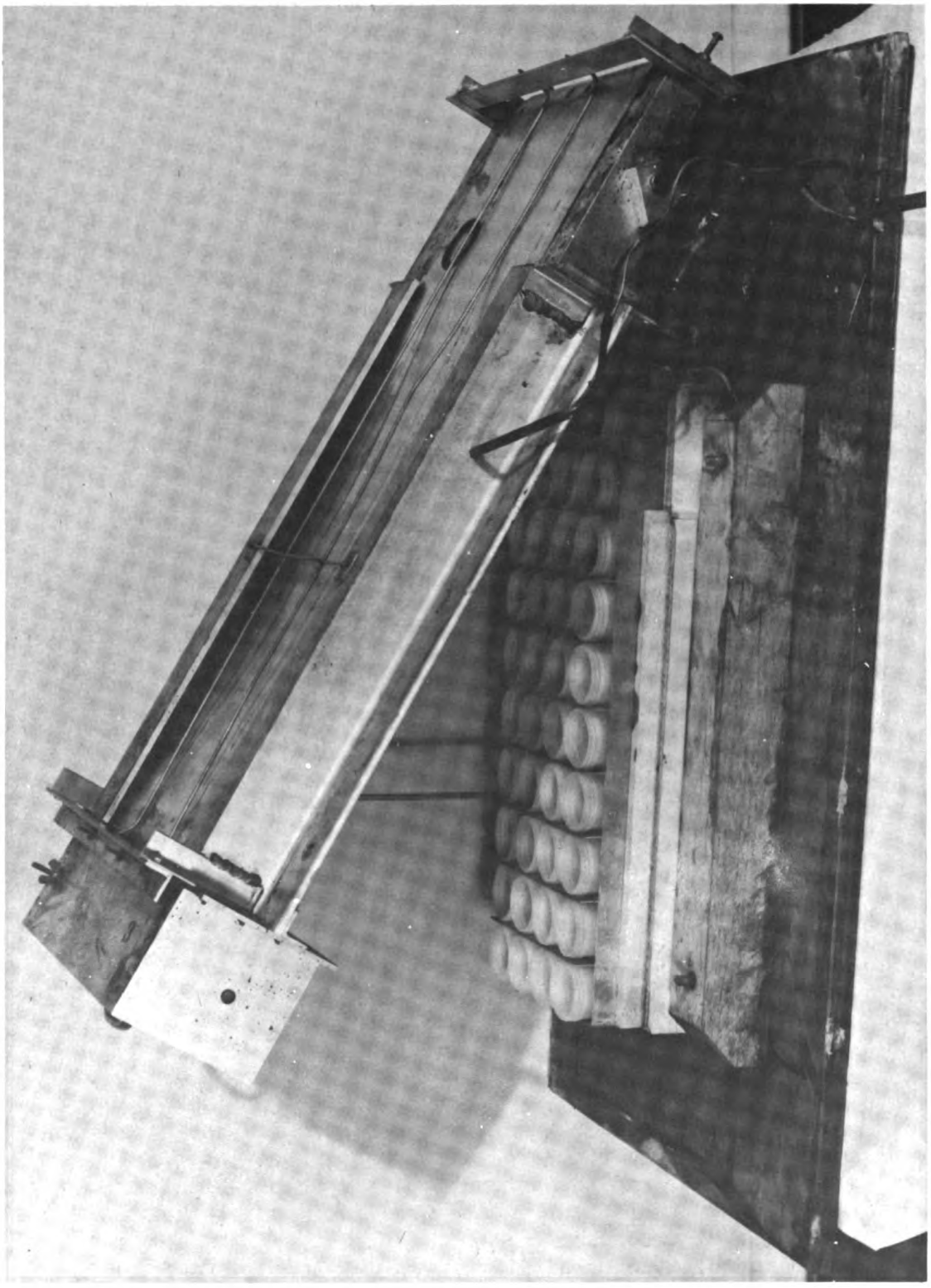

Fig. 3.2 Differential Fallout Collector

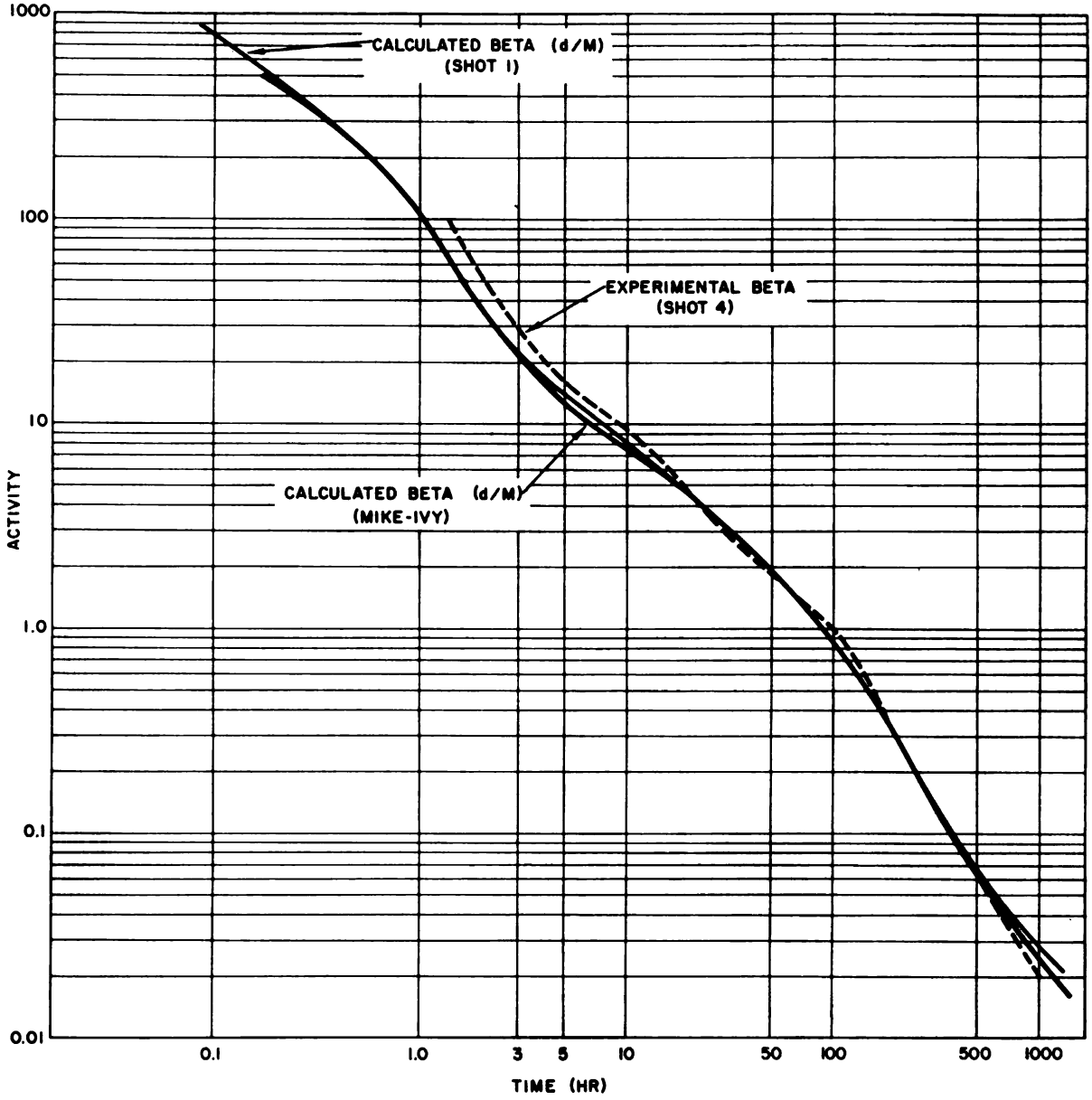

Fig. 5.1 Experimental and Calculated Beta Decay Curves

[redacted]

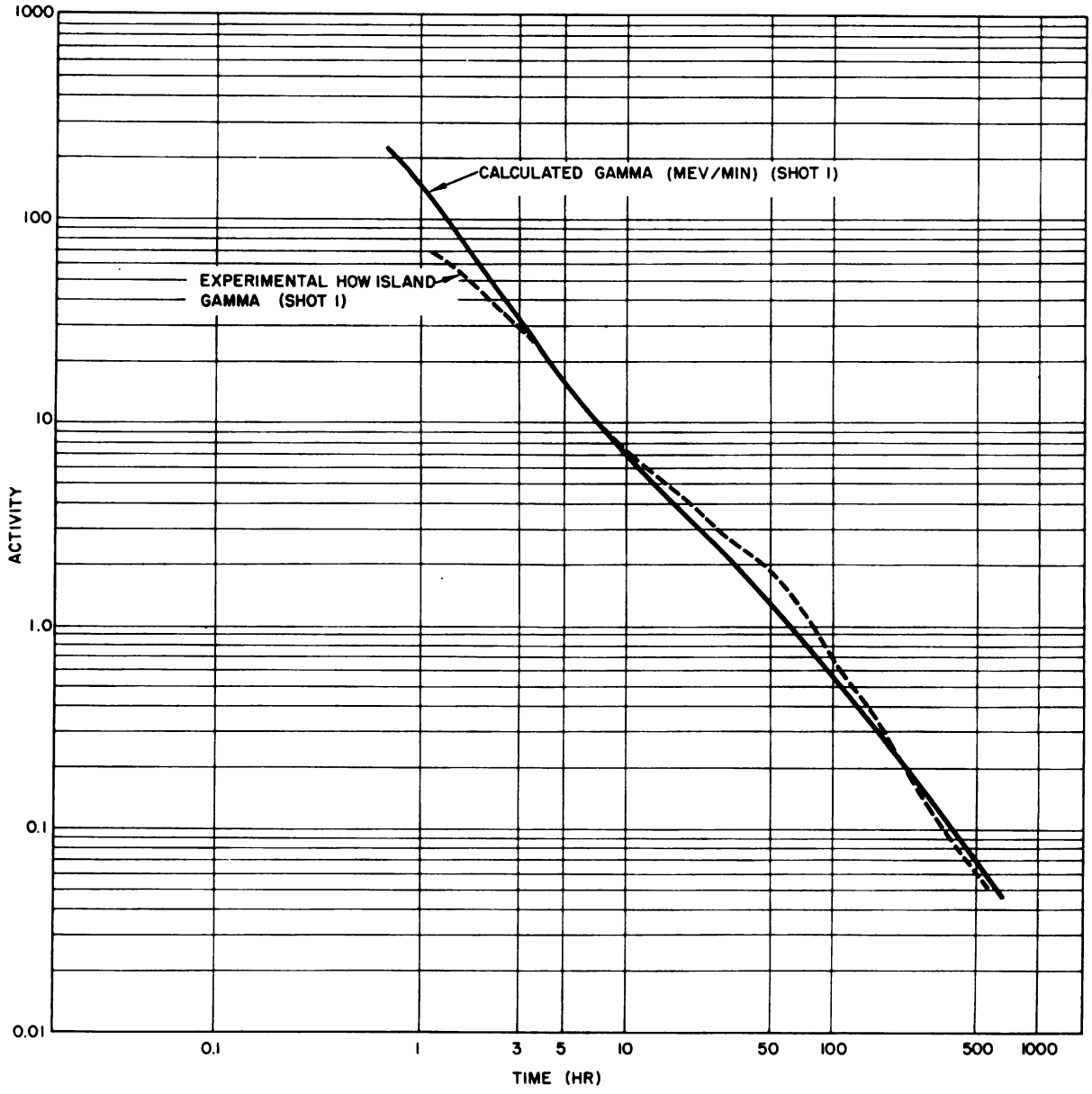

Fig. 5.2 Calculated Gamma Decay Curve and Experimental Gamma Ionization Decay Curve for Shot 1

[redacted]

small. No samples suitable for particle analysis were obtained from Shot 3. Following Shot 1, 6971 radioactive particles were analyzed from the area within the Bikini Atoll and 621 particles collected on the outer atolls of Ailinginae, Rongelap, and Utirik were evaluated. The differential fallout collector on the island of Alice contained some particulate from Shot 6. These data are also presented.

5.2.1 Shot 1, Close-in Fallout

The size distribution of close-in fallout particles with respect to time for four lagoon and three island stations are given in Appendix C. Only radioactive particles are included in the data. Of the 40 available sampling increments within each differential collector, those increments that visually appeared to contain a large amount of particulate were selected for analysis. Increments over a wide time period were likewise selected. Analysis of the bar graphs with respect to rate of arrival or time of arrival is therefore an approximation. Data on time of arrival are presented in Section 5.6 of this report.

Figure 5.4 shows the size frequency distribution of the Shot 1 close-in particulate. It is a composite of the bar graphs for the four lagoon and three island stations. (Figs. C-1 through C-7.)

Figure 5.5 is a plot of the cumulative size distribution of Shot 1 particulate presented on a log probability graph. The size distribution is very close to log normal with a geometric mean particle diameter of 112 μ.

5.2.2 Shot 1, Outer Island Fallout

Samples of earth were collected by the outer island survey team following Shot 1.[15] The radioactive particulate found in these soil samples was analyzed for size distribution and the results are presented in Fig. 5.6. These atolls were 70 to 280 nautical miles from Shot 1. Figure 5.7 shows a log normal size distribution for particles collected on three atolls. The geometric mean particle diameters are presented in Table 5.4.

TABLE 5.4 - Geometric Mean Particle Diameter

Atoll	Distance from Shot Point (n mi)	Geometric Mean Particle Diameter (μ)
Bikini	10	112
Ailinginae	70	60
Rongelap	107	70
Utirik	277	45

[redacted]

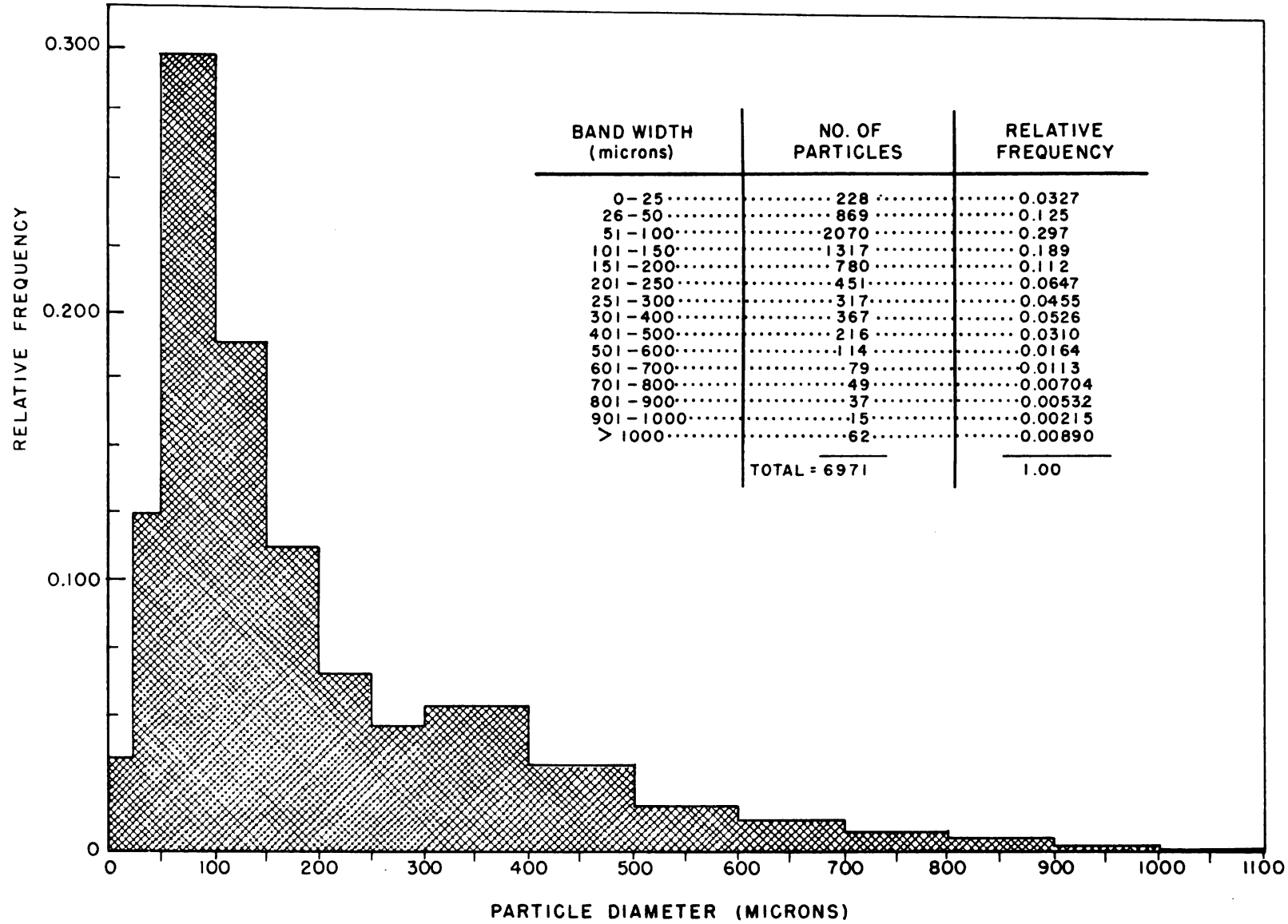

BAND WIDTH (microns)	NO. OF PARTICLES	RELATIVE FREQUENCY
0 – 25	228	0.0327
26 – 50	869	0.125
51 – 100	2070	0.297
101 – 150	1317	0.189
151 – 200	780	0.112
201 – 250	451	0.0647
251 – 300	317	0.0455
301 – 400	367	0.0526
401 – 500	216	0.0310
501 – 600	114	0.0164
601 – 700	79	0.0113
701 – 800	49	0.00704
801 – 900	37	0.00532
901 – 1000	15	0.00215
> 1000	62	0.00890
	TOTAL = 6971	1.00

Fig. 5.4 Shot 1, Composite Particle Size Distribution

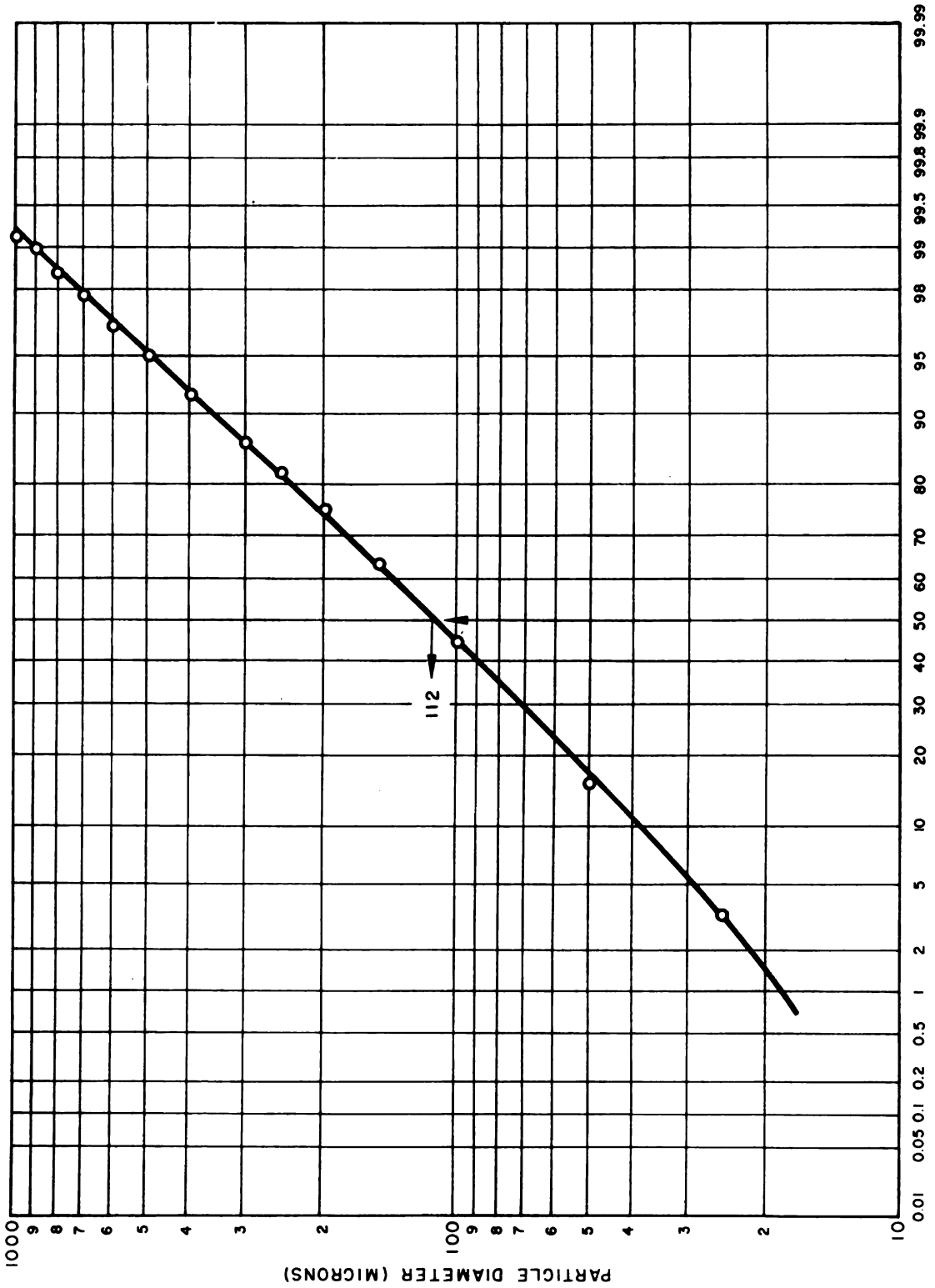

Fig. 5.5 Shot 1, Cumulative Particle Size Distribution

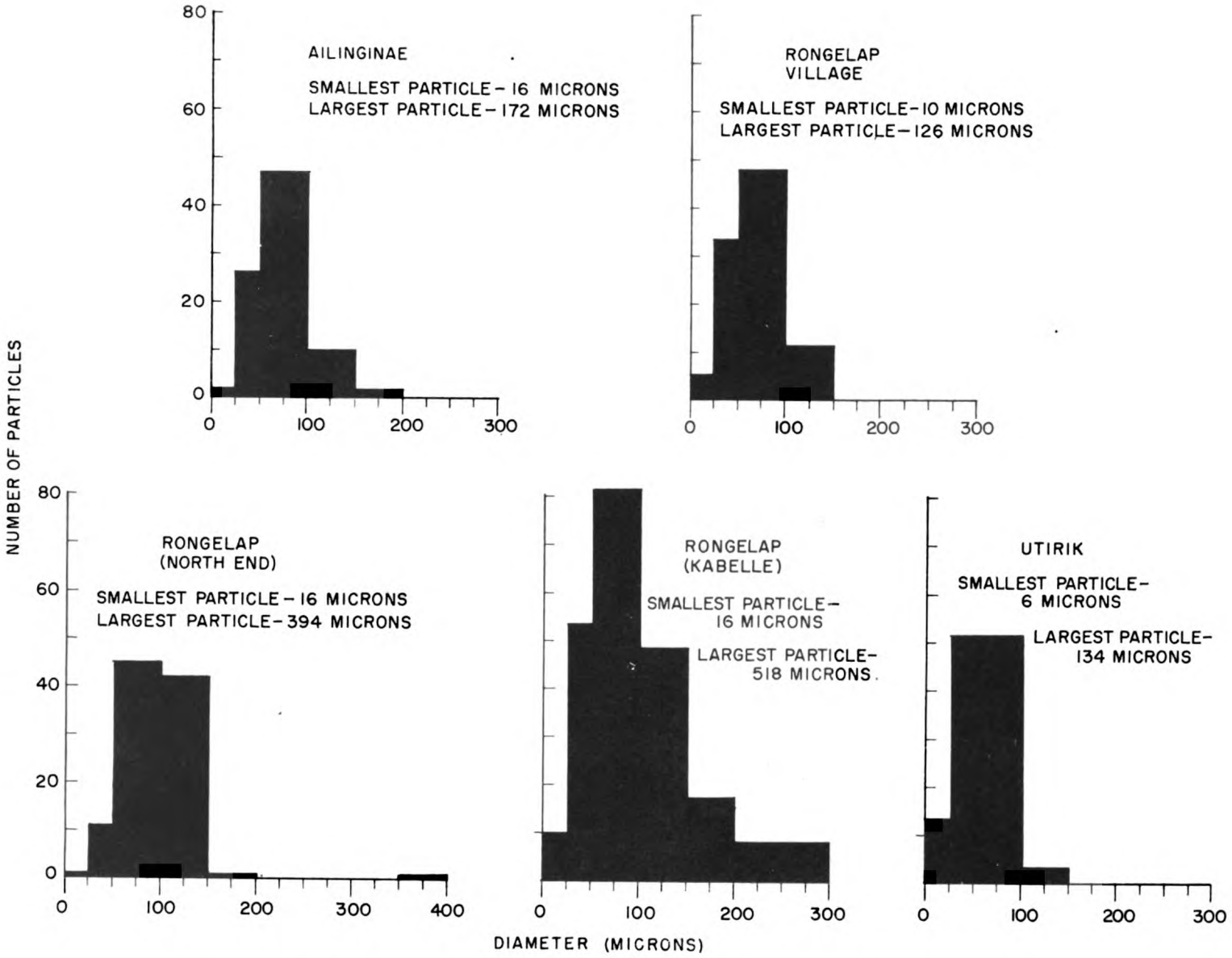

Fig. 5.6 Shot 1, Outer Atoll Particle Size Distribution

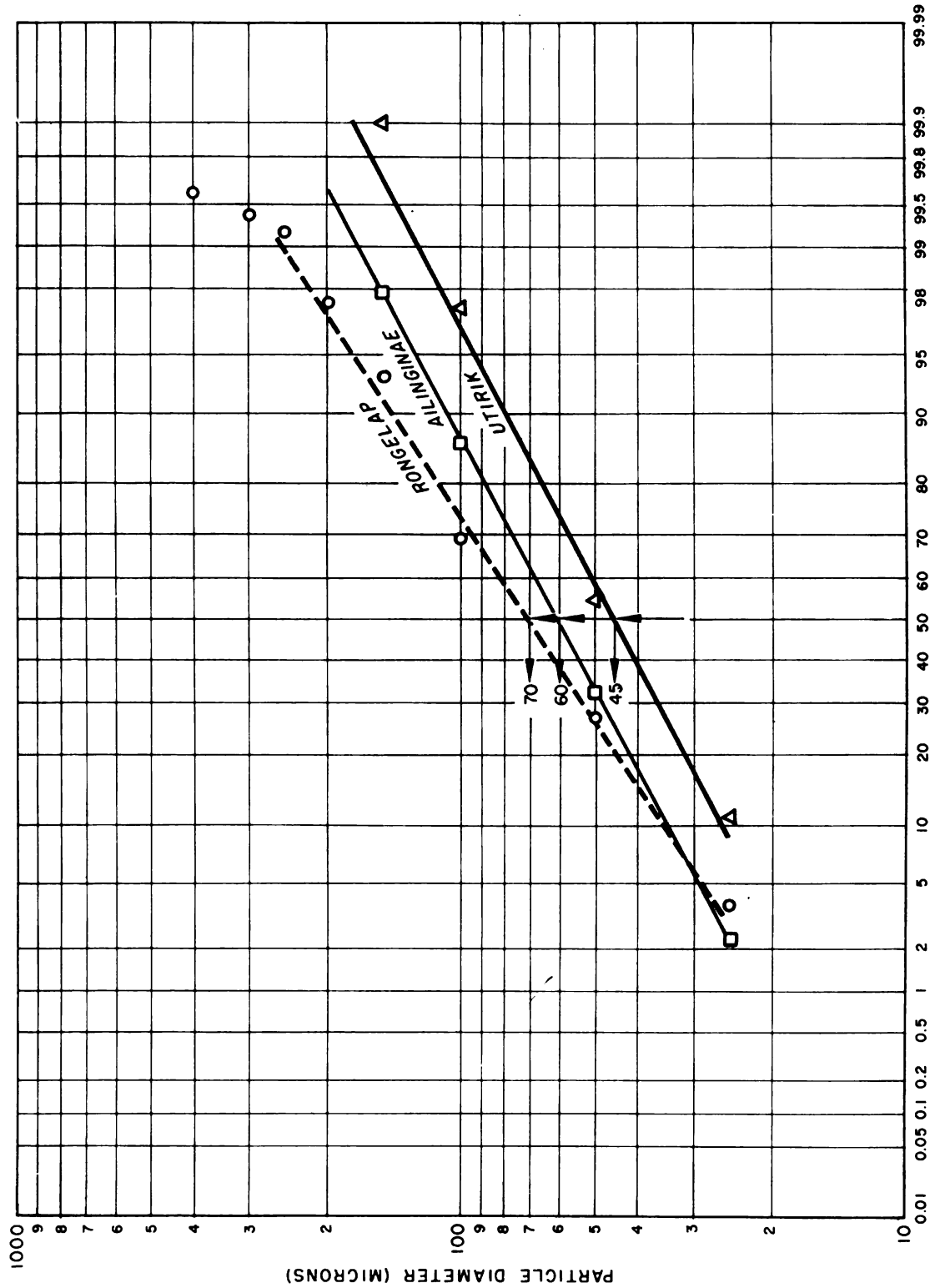

Fig. 5.7 Shot 1, Outer Atoll Cumulative Particle Size Distribution

[redacted]

The fact that the mean particle diameter at Ailinginae is smaller than at Rongelap can be partially explained by analysis of the wind profile which indicates, as one moves south from the axis of symmetry of the fallout pattern, that the particles delivered have smaller diameters (see Chapter 6).

5.2.3 Shot 6, Particle Size

The differential collector stationed on Alice contained visible particulate as well as some liquid; the analysis of particle size distribution is presented in Appendix C. With a total of 321 particles measured the distribution was nearly log normal with a geometric mean diameter of 180 μ as shown in Fig. 5.8. Alice was 3 nautical miles from ground zero.

5.3 RATIO OF ACTIVE TO INACTIVE PARTICLES

One of the most difficult problems to resolve is the ratio of active to inactive fallout particles that arrive at a collecting instrument. This is especially true of the smaller diameter particles because it is extremely difficult to avoid pollution of the sample by extraneous particulate. In this analysis many small inactive particles were observed during the measurement of particle diameters. In many cases these particles were less than 5 μ in diameter. To arrive at a ratio, all particulate was ignored that did not have the characteristic white opaque color of fallout.

Two samples were analyzed from Shot 1 fallout collected at lagoon stations where the effect of island dust pollution was minimized. The results are shown in Fig. 5.9. Approximately 25 per cent of the particles were found to be inactive with the mean particle size of the inactive particles smaller than the active.

5.4 PARTICLE DENSITY

Particles from the Shot 1 lagoon station differential fallout collectors were analyzed to determine their apparent density which is defined as the specific gravity of the particle as a whole. Because of the station locations and the collecting instrument used, these particles had a very high probability of being true fallout. Seventy-nine particles from stations 250.04, 250.17, and 250.24 were measured. Density, average diameter, color, and relative activity were determined for each particle.

Table 5.5 shows the particle density found at each station. The overall average density of the 79 particles was 2.36 g/cu cm with a standard deviation of 8.9 per cent.

Attempts to find relationships between particle size and activity; particle size and density; and density and activity proved unsuccessful. All particle density data are tabulated in Appendix D.

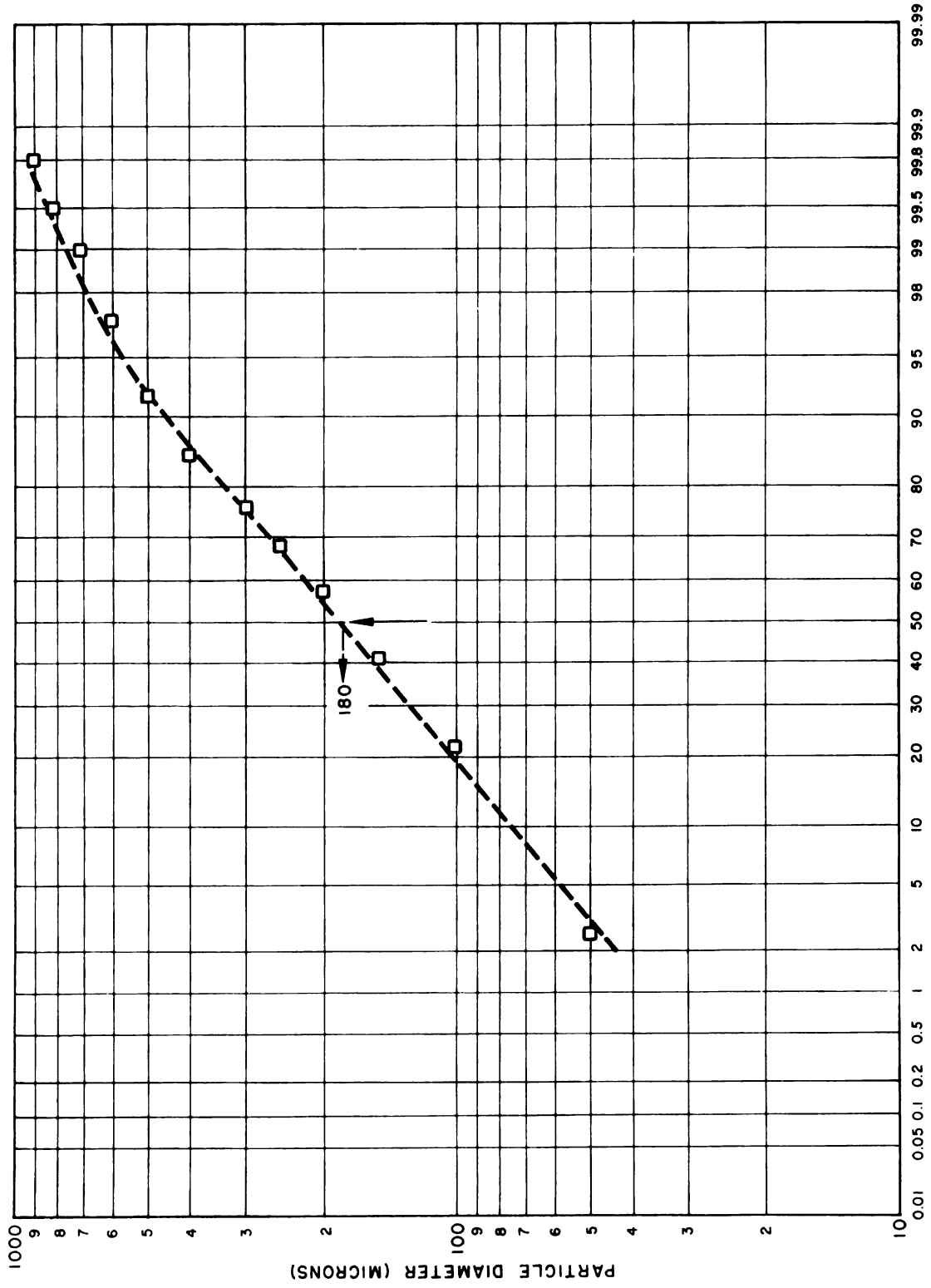

Fig. 5.8 Shot 6, Cumulative Particle Size Distribution, Station Alice

[redacted]

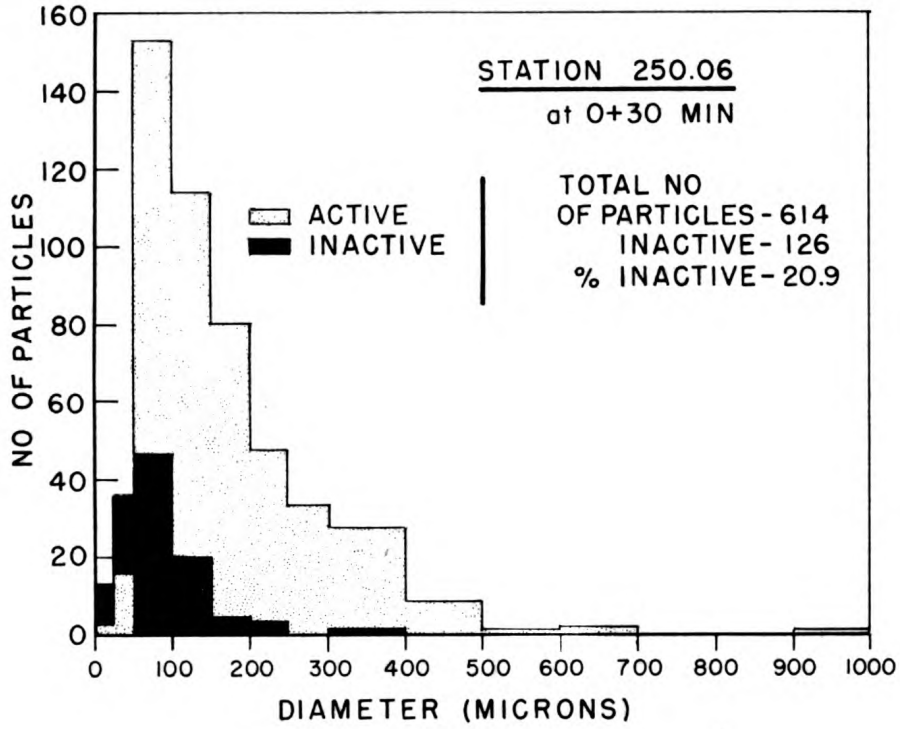

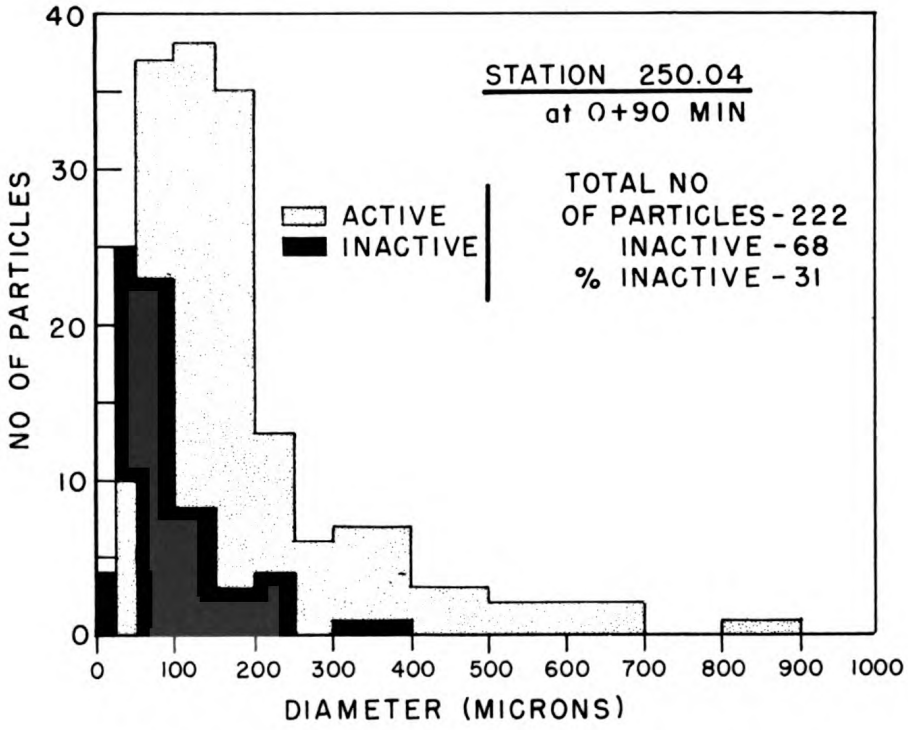

Fig. 5.9 Shot 1, Ratio of Active to Inactive Particles

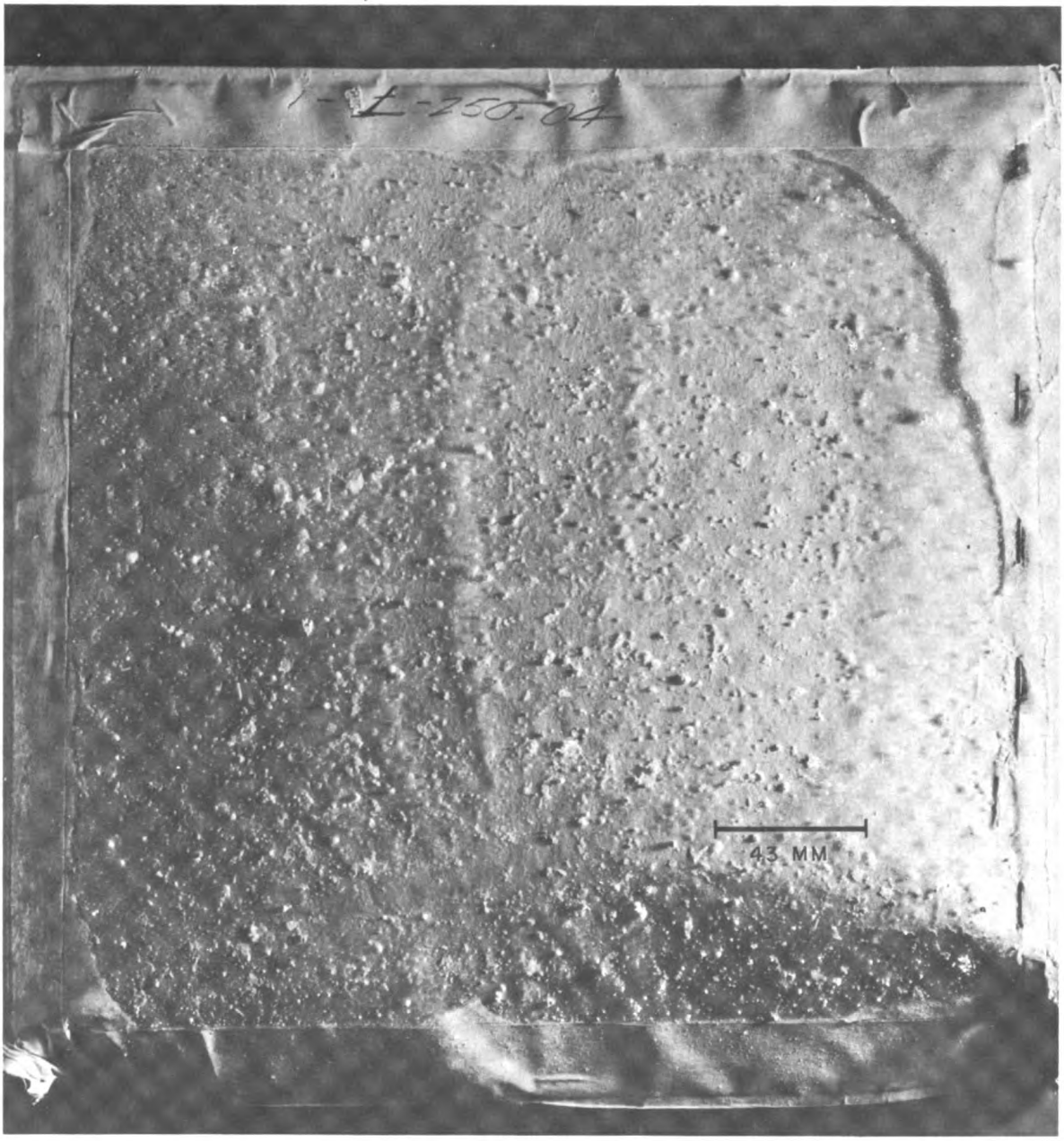

Fig. 5.10 Shot 1, Fallout Particulate, Station 250.04

[redacted]

Analysis of the gamma time-intensity recorder trace located at How gave the best evidence of the rate of arrival of fallout.

Use of the differential fallout collector and the time-intensity recorder for determining the period of fallout was restricted to the lagoon and islands of Bikini Atoll thereby limiting the distance to 15 nautical miles. The average arrival time within the area was 0 + 28 min with cessation averaging 0 + 117 min resulting in an average period of 89 min. These data compare well with that observed at IVY[1] where the period was somewhat less than 2 hr. Residual fallout which was of such quantity that it contributed little to the overall field was found to deposit for a period of several hours after the deposition of the main body of material.

The Bikini Atoll islands along the axis of the fallout pattern experienced fallout over a longer period of time than did those islands located in a crosswise direction.

5.6.2 Shot 2

No evidence was found of primary fallout at early times in the Bikini Lagoon. Secondary fallout of maximum intensity of 40 mr/hr arrived at How Island 37.5 hr after Shot 2, as shown by the gamma time-intensity recorder.

5.6.3 Shot 3

No differential fallout collectors were operative for Shot 3. The gamma time-intensity recorder at How Island indicated a time of arrival of 0 + 38 min. Project 2.2 established an arrival time on Dog Island of approximately 0 + 20 min.[2]

5.6.4 Shot 6

One differential fallout collector located at Alice Island, Eniwetok Atoll, received significant fallout and indicated an arrival time of 0 + 35 min with the period of fallout being 65 min (Fig. C-18).

5.7 RATE OF ARRIVAL OF FALLOUT AND INTEGRATED DOSE

Of the two gamma ionization time-intensity recorders installed on Yoke and How Islands of Bikini Atoll, only the one on How survived and recorded data from Shots 1, 2, and 3. These data give accurate information on rate of arrival of fallout as well as time of arrival.

5.7.1 Rate of Arrival

Table 5.7 presents the time of arrival of fallout and time of peak activity for Shots 1, 2, and 3. The time at which the activity peaks is not the time of cessation of fallout. It is best described as the time at which the rate of decay is greater than the rate of build-up of fallout.

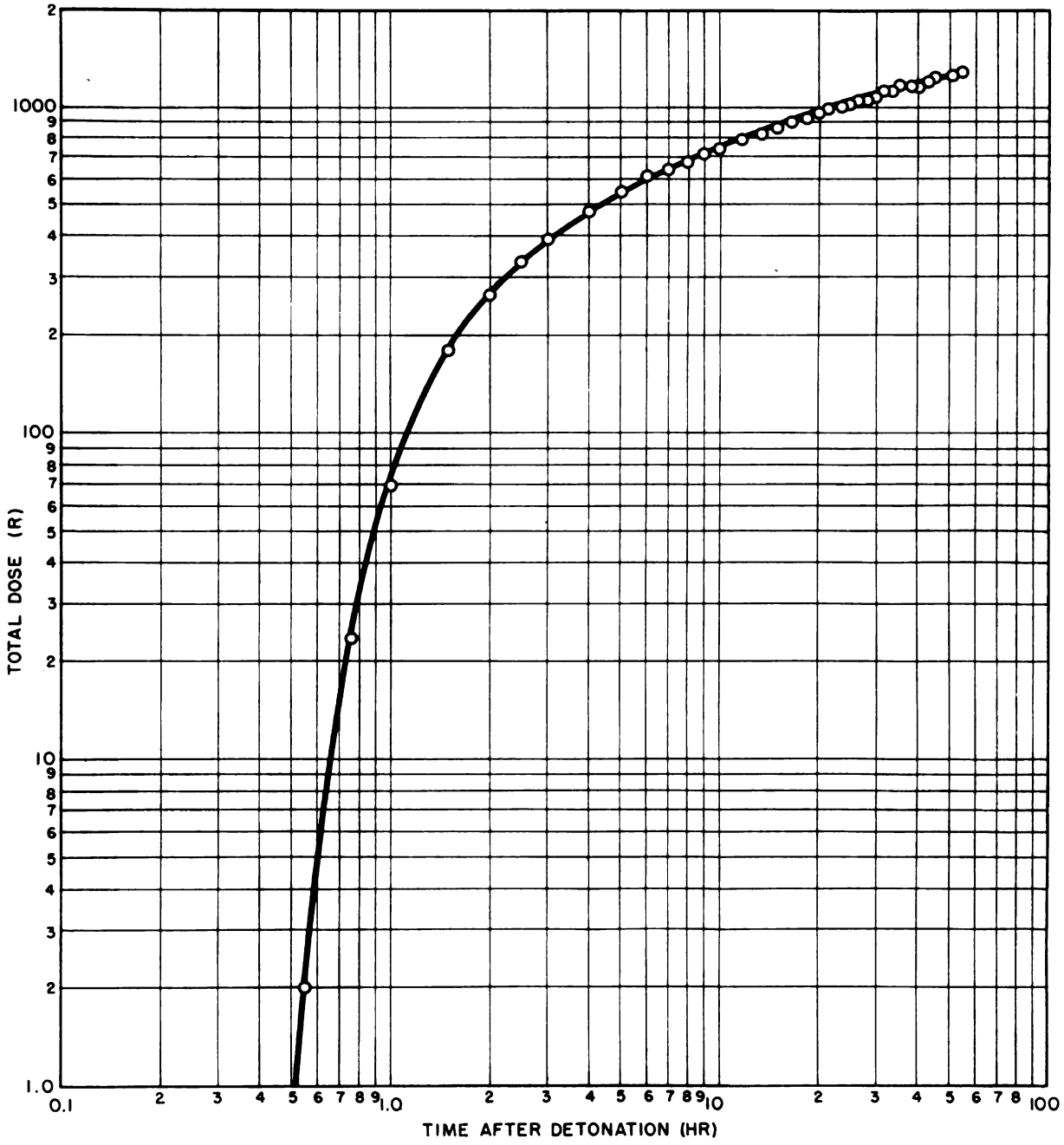

Fig. 5.11 Shot 1, Integrated Gamma Dose, Station 251.03

[redacted]

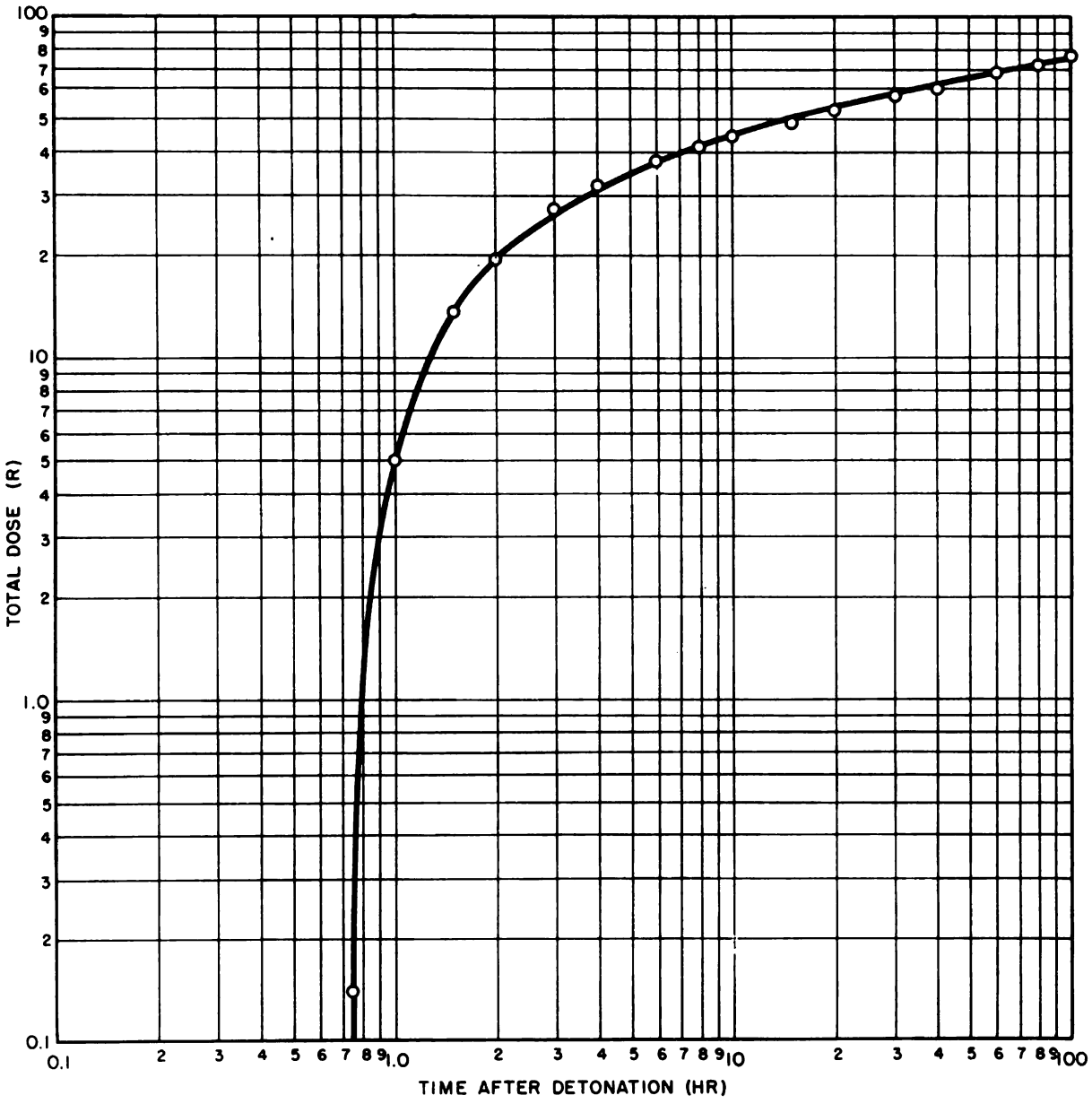

Fig. 5.12 Shot 3, Integrated Gamma Dose, Station 251.03

[redacted]

TABLE 5.7 - Rate of Arrival of Fallout

Shot	Station	Time of Arrival (min)	Time to Peak Activity (min)	Time Between Fallout Arrival and Peak Activity (min)
1	How Island	0 + 15	0 + 65	50
3	How Island	0 + 38	0 + 66	28
2 (secondary fallout)	How Island	0 + 2250	0 + 3280	1030

5.7.2 Total Dose

Figures 5.11 and 5.12 indicate the integrated gamma dose to a time approximately 100 hr after detonation for Shots 1 and 3. Shot 2 deposited only secondary fallout on How Island and the data are not presented.

[redacted]

applied to the samples collected at the lagoon stations, thereby permitting estimation of infinite field levels for those locations. Using the total collector as the primary source of data, gamma field contours were thus constructed. Where total collector data were missing, activity levels obtained from the gummed paper collectors were used. All data presented are based on the levels of activity that would have existed had the fallout deposited on an infinite land plane.

The fields as indicated by the film badges were erratic. Because of poor location of the film badges during sampling and unsatisfactory history during and after recovery, these data are not considered in this analysis.

6.1.1 Shot 1

Table 6.1 shows correlation among the data obtained by survey measurements on Bikini Atoll and data obtained from the total collectors and gummed paper collectors located there. All measurements have been converted to r/hr at 1 hr for comparisons.

Figure 6.1 is an isodose rate plot of gamma activity over the atoll. There is indication of a very steep gradient from north to south across the lagoon. This gradient is also indicated in the analysis of Shot 1 particle trajectory data as illustrated in Fig. 6.5.

TABLE 6.1 - Shot 1, Gamma Infinite Field Levels at Bikini Atoll Converted to r/hr at 1 hr as Determined by Various Techniques

Station	Code	Measured by Rad Safe	Measured by Proj. 2.5a	Total Collector Analysis	Gummed Paper Analysis
251.02	Fox	1920	1390	1630	-
251.03	How	510	690	725	528
251.04	Love	270	415	450	-
251.05	Nan	213	208	266	-
251.06	Oboe	76	45	51	-
251.07	Uncle	25	17	18	31
251.08	William	21	17	28	26
251.09	Yoke	-	-	-	-
251.10	Zebra	38	21	23	-
250.04	Lagoon	-	-	113	-
250.05	Lagoon	-	-	68	112
250.06	Lagoon	-	-	-	86
250.17	Lagoon	-	-	-	60
250.18	Lagoon	-	-	9.4	-
250.22	Lagoon	-	-	7.5	50
250.24	Lagoon	-	-	20	-

[redacted]

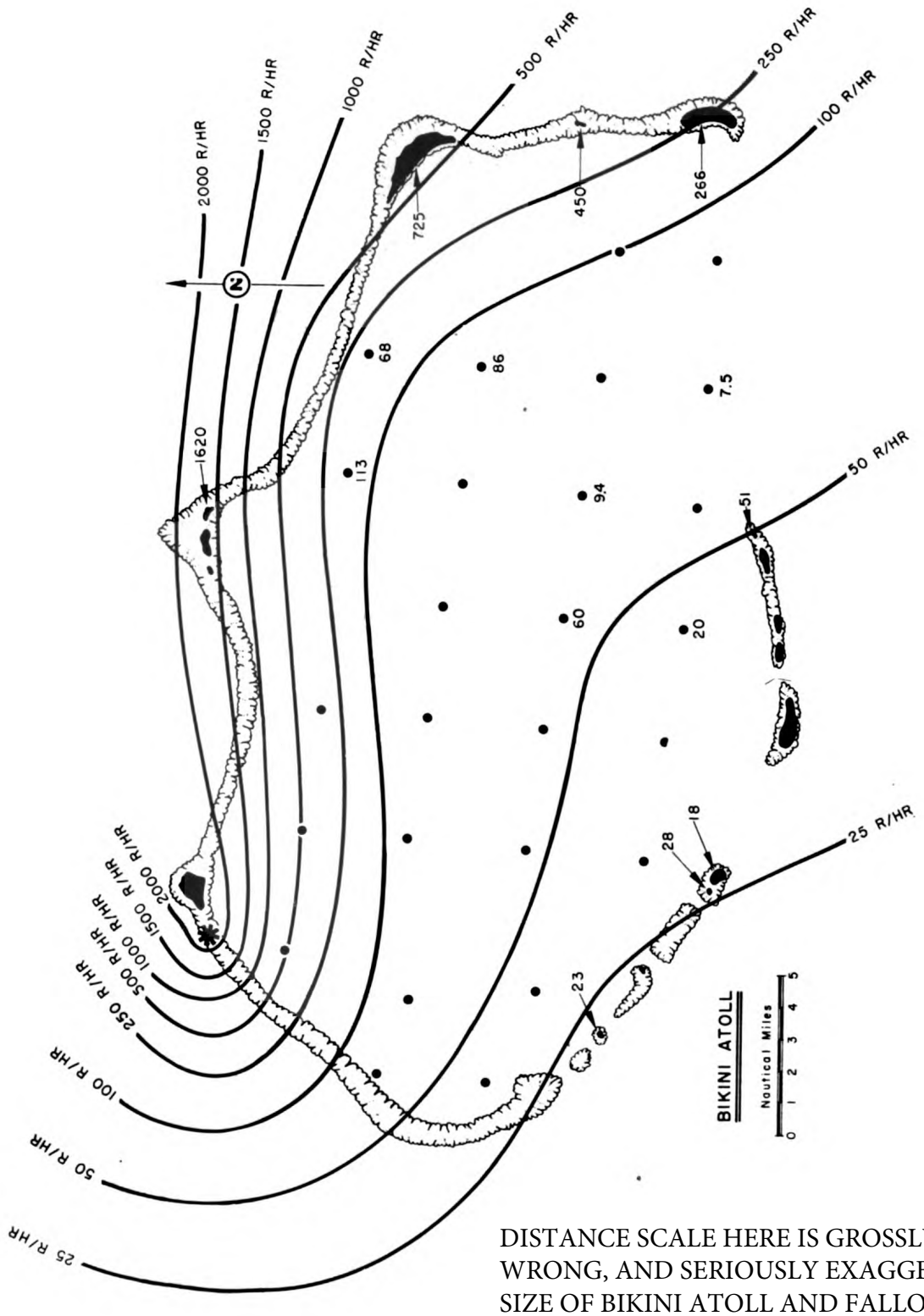

Fig. 6.1 Shot 1, Close-in Gamma Fallout Pattern (r/hr at 1 hr)

DISTANCE SCALE HERE IS GROSSLY WRONG, AND SERIOUSLY EXAGGERATES SIZE OF BIKINI ATOLL AND FALLOUT PATTERN!

[redacted]

6.1.2 Shot 3

The Shot 3 pattern was well defined because the direction* of fallout crossed the collecting array perfectly. The highest measured level of gamma activity was 360 r/hr at 1 hr at Station 250.17 (see Table 6.2). Figure 6.2 presents the gamma fallout pattern in r/hr at 1 hr.

TABLE 6.2 - Shot 3, Gamma Infinite Field Levels at Bikini Atoll Converted to r/hr at 1 hr as Determined by Various Techniques

Station	Code	Measured by Rad Safe	Measured by Proj. 2.5a	Total Collector Analysis	Gummed Paper Analysis
251.02	Fox	158	-	98	107
251.03	How	16	33	25	20
251.04	Love	3.2	3.3	3.4	-
251.08	William	4.5	-	8.1	-
251.10	Zebra	2.8	1.4	4.2	1.9
250.01	Lagoon	-	-	5.1	-
250.02	Lagoon	-	-	4.2	-
250.05	Lagoon	-	-	107	103
250.06	Lagoon	-	-	62	39
250.07	Lagoon	-	-	64	84
250.08	Lagoon	-	-	33	-
250.09	Lagoon	-	-	4.5	-
250.12	Lagoon	-	-	0.9	-
250.13	Lagoon	-	-	1.5	-
250.14	Lagoon	-	-	2.7	-
250.15	Lagoon	-	-	2.4	-
250.16	Lagoon	-	-	49	65
250.17	Lagoon	-	-	340	360
250.18	Lagoon	-	-	203	201
250.19	Lagoon	-	-	8.5	2.3
250.22	Lagoon	-	-	7	-

6.1.3 Shot 4

The direction* of fallout limited gamma levels of military significance to the northern islands of the atoll. The majority of the lagoon stations were in the fringe area of the fallout pattern. Figure 6.3 and Table 6.3 indicate the extent of the gamma fallout in r/hr at 1 hr for Shot 4.

---

* Determined from wind data.

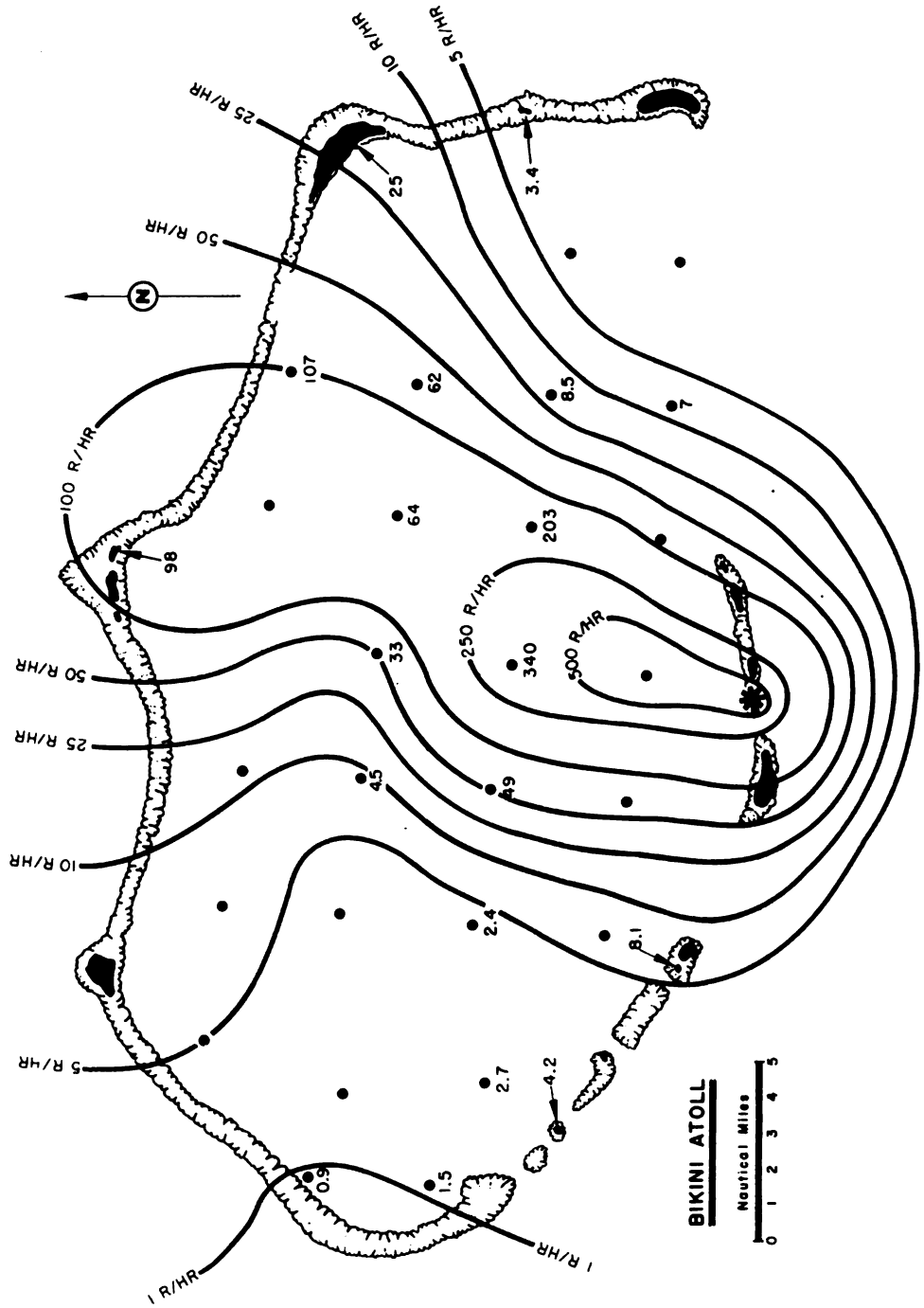

Fig. 6.2 Shot 3, Close-in Gamma Fallout Pattern (r/hr at 1 hr)

DISTANCE SCALE HERE IS GROSSLY WRONG, AND SERIOUSLY EXAGGERATES SIZE OF BIKINI ATOLL AND FALLOUT PATTERN!

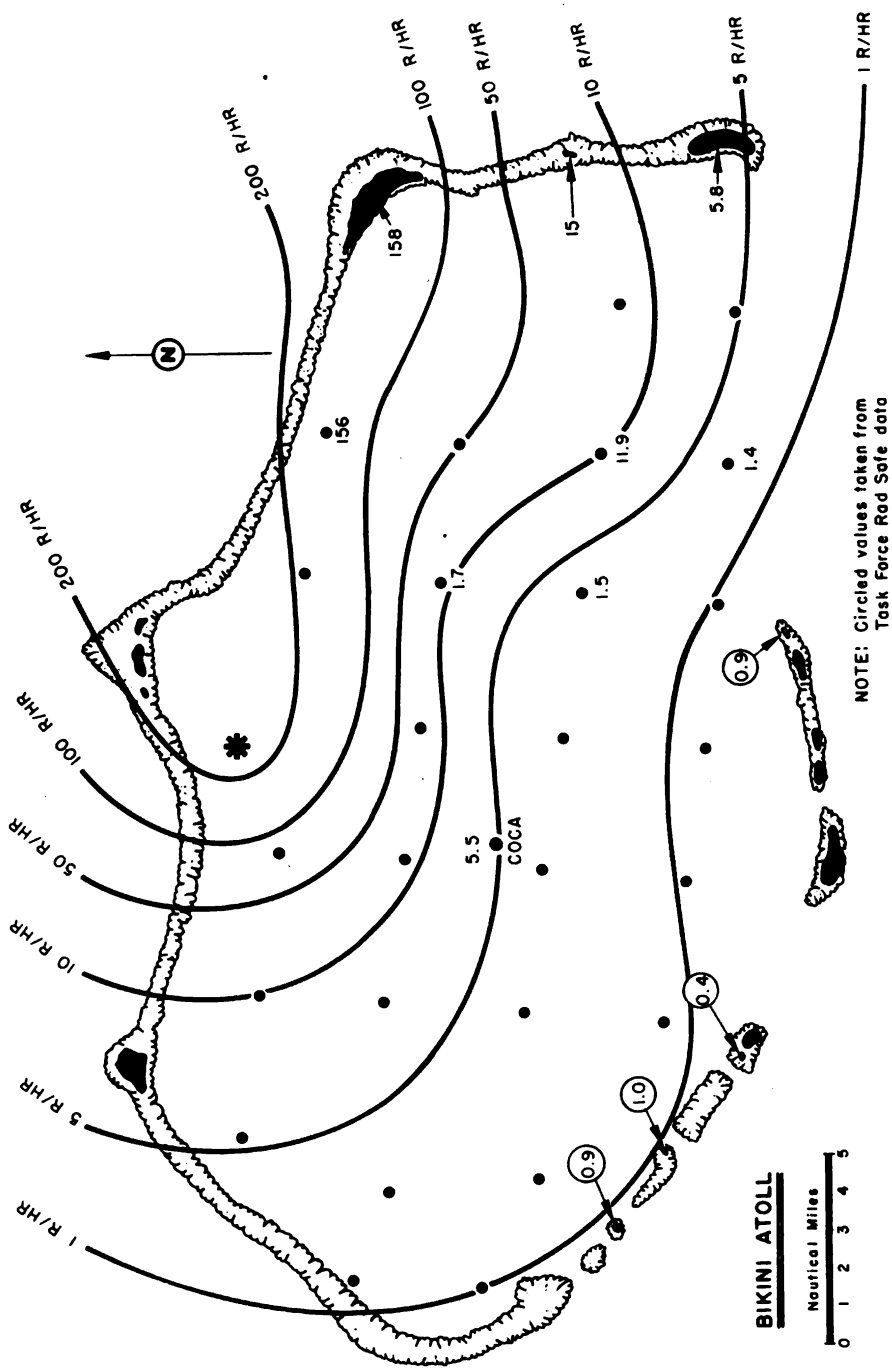

Fig. 6.3 Shot 4, Close-in Gamma Fallout Pattern (r/hr at 1 hr)

DISTANCE SCALE HERE IS GROSSLY WRONG, AND SERIOUSLY EXAGGERATES SIZE OF BIKINI ATOLL AND FALLOUT PATTERN!

[redacted]

TABLE 6.3 - Shot 4, Gamma Infinite Field Levels at Bikini Atoll Converted to r/hr at 1 hr as Determined by Various Techniques

Station	Code	Measured by Rad Safe	Measured by Proj. 2.5a	Total Collector Analysis	Gummed Paper Analysis
251.03	How	128	300	158	-
251.04	Love	15	26	15	-
251.05	Nan	5	4.7	5.8	4.7
251.06	Oboe	0.9	0.8	-	-
251.08	William	-	0.4	-	-
251.09	Yoke	-	1.0	-	-
251.10	Zebra	-	0.9	-	-
250.05	Lagoon	-	-	156	222
250.07	Lagoon	-	-	1.7	0.9
250.18	Lagoon	-	-	1.5	-
250.19	Lagoon	-	-	11.9	1.9
250.22	Lagoon	-	-	1.4	1.3
Coca	Lagoon	-	-	5.5	-

6.1.4 Shot 6

A very complete array of collecting instruments was employed for Shot 6 in the Eniwetok Lagoon and on the atoll islands. Since the fallout went in a northerly direction from shot point very few of the stations received significant fallout. The island of Alice, approximately 3 nautical miles from surface zero, was contaminated to 45 r/hr at 1 hr as indicated in Table 6.4.

The fallout collected was primarily upwind fallout with the gamma field pattern defined in Fig. 6.4. The relatively low levels about surface zero fit well with the overall contours as determined by Project 2.7.

6.2 EXTENDED FALLOUT PATTERN FOR SHOT 1

The contamination of the outlying atolls[15] to the east of Bikini and the measured values of the levels of residual gamma activity following Shot 1 offered an excellent opportunity to evaluate the fallout pattern resulting from a super weapon. A complete analysis of Shot 1 fallout based on available field readings and a comprehensive analysis of the wind structure with respect to its effect on particle trajectories is presented.

6.2.1 Measured Field Values of Residual Gamma Activity

The measured values of residual gamma activity obtained by H. Scoville, [15] were converted to r/hr at 1 hr using the composite gamma ionization decay curve, Fig. 5.3. One hour post detonation is simply a convenient reference; as will be noted in later sections,

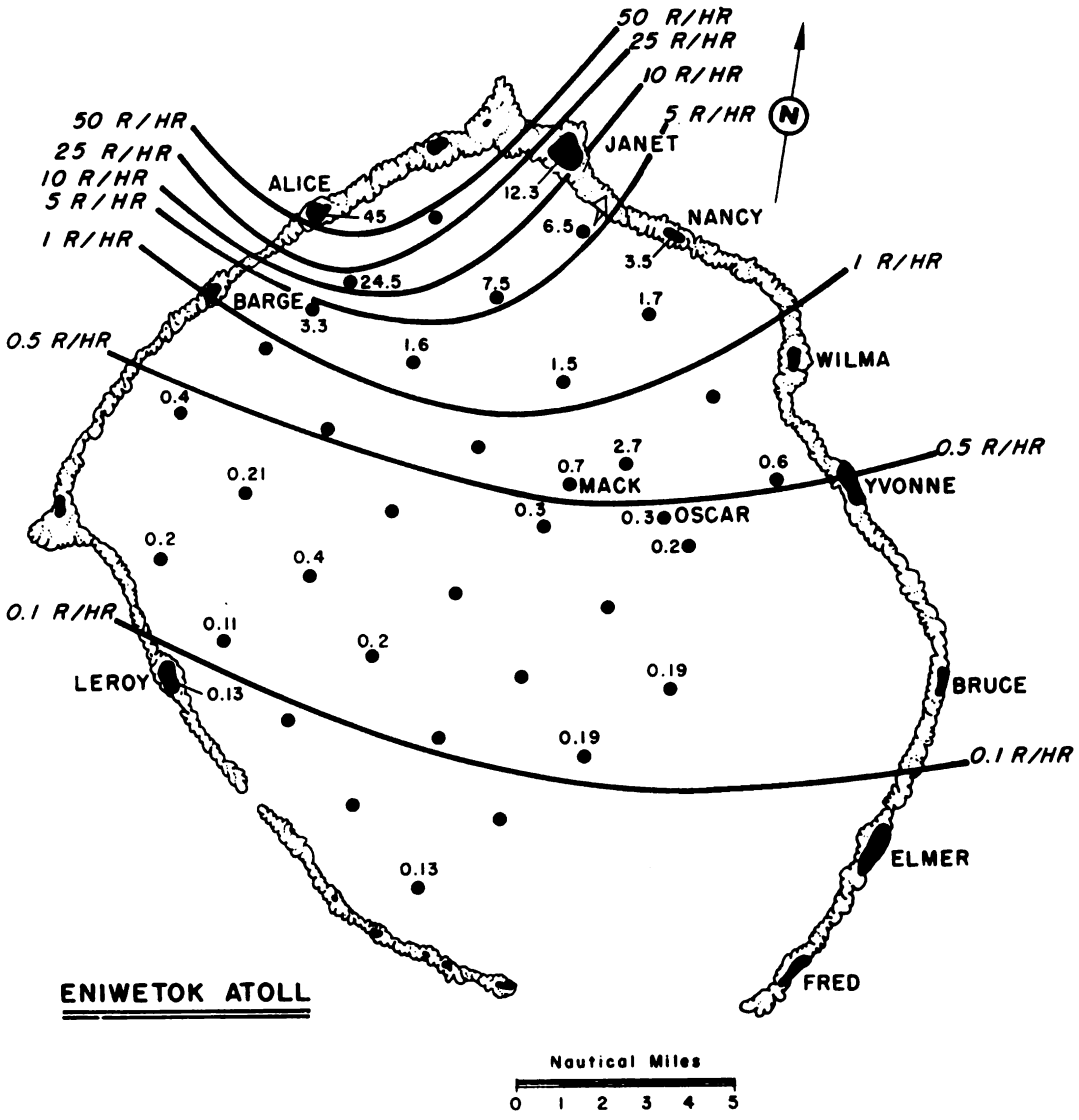

Fig. 6.4 Shot 6, Close-in Gamma Fallout Pattern (r/hr at 1 hr)

TABLE 6.4 - Shot 6, Gamma Infinite Field Levels at Eniwetok Atoll Converted to r/hr at 1 hr as Determined by Various Techniques

Station	Code	Measured by Rad Safe	Measured by Proj. 2.5a	Total Collector Analysis	Gummed Paper Analysis
	Alice	26	42	45	-
	Janet	4.7	5.8	12.3	-
	Leroy	-	-	0.13	-
	Nancy	-	3.3	3.5	-
250.27	Lagoon	-	-	6.5	-
250.28	Lagoon	-	-	1.7	-
250.30	Lagoon	-	-	0.6	-
250.32	Lagoon	-	-	7.5	-
250.33	Lagoon	-	-	1.5	-
250.34	Lagoon	-	-	2.7	-
250.35	Lagoon	-	-	0.2	-
250.36	Lagoon	-	-	24.5	-
250.37	Lagoon	-	-	1.6	-
250.39	Lagoon	-	-	0.3	-
250.41	Lagoon	-	-	0.19	-
250.47	Lagoon	-	-	0.19	-
250.48	Lagoon	-	-	0.4	-
250.49	Lagoon	-	-	0.21	-
250.50	Lagoon	-	-	0.4	-
250.51	Lagoon	-	-	0.2	-
250.54	Lagoon	-	-	0.2	-
250.55	Lagoon	-	-	0.11	-
250.58	Lagoon	-	-	0.13	-
MAC-1	Lagoon	-	-	0.7	-
Barge	Lagoon	-	-	8.3	-
Oscar	Lagoon	-	-	0.3	-

fallout first arrived at the outlying atolls several hours after detonation. These data (Table 6.5), along with the measurements made within the Bikini Atoll as shown in Fig. 6.1, represent the available gamma field measurements used in this analysis.

6.2.2 Determination of Experimental Model - Shot 1

Although significant gamma field data were obtained, they fell far short of completely defining the fallout pattern. However, with the added knowledge of the axis of symmetry of the fallout pattern,

TABLE 6.5 - Shot 1 Residual Gamma Activity on Outer Islands

Location	Gamma Activity r/hr at 1 hr
Ailinginae	
Enibuk	92.5
Sifo	77
Bokonikaiaru	108
Rongelap	
Naen	2420
Arrik	1950
Lomuilal	1950
Gejen	1950
Lukuen	1160
Eriirippu	1480
Kabelle	1050
Anidjet	737
Enialo	264
Bosch	342
Rongelap	197
Arqar	132
Eniran	316
Rongerik	
Bok	770
Latoback	385
Mortlook	347
Rongerik	308
Eniwetak	216
Utirik	
Aon	26.6
Utirik	20
Bikar	
Bikar	93.3

gamma field contours were constructed. This information was obtained by completely analyzing the wind structure existing at and after shot time with respect to its effect on fallout particles originating in the stem and cloud. To establish a pattern on this basis it was necessary to make the following assumptions:

(a) The relative contribution of particles less than 25 μ in diameter to the residual gamma field defining the area of primary fallout was negligible.

(b) The particle size distribution is the same at all elevations and homogeneous throughout the visible dimensions of the cloud and stem. This assumption was arbitrarily chosen as the best

approximation to the actual case. Consideration of the extreme vertical velocities and violent turbulence existing within the cloud before stabilization makes it appear unlikely that any major fractionation of particle size would occur within the cloud and stem at early times. However, any error introduced in the resultant axis of symmetry as a consequence of this assumption would be minor because of the particular wind situation throughout Shot 1 fallout.

(c) A vertical line from ground zero to the maximum elevation of the cloud represents the axis of symmetry of the stem and cloud.

(d) The physical dimensions of the cloud and stem can be satisfactorily represented by assuming they define cylinders about the vertical axis of symmetry of the detonation.

The above assumptions defined a simplified model of the Shot 1 cloud from which, with information obtained experimentally and the complete wind data, the particle trajectories were calculated and their points of intersection with the surface of the earth determined as well as were particle transit times.

6.2.3 Experimental Data Applied to Model Evaluation

The following experimental data were used to complete this analysis:

(a) From the particle size analysis of the Bikini Atoll and outer island atoll fallout, (see Section 5.2) it was determined that the particulate were almost entirely irregular in shape.

(b) The average apparent density of these particles was determined to be 2.36 g/cu cm as discussed in Section 5.4.

(c) The size distribution of the fallout particulate ranged between 2000 and 25 μ in diameter.

(d) The cloud dimensions both vertical and horizontal were obtained by cloud photography.5/

(e) Meteorological data of the variation with height of both the wind direction and speed, and the air temperature were obtained from the Task Force Weather Central.

6.2.4 Determination of Particle Trajectories

From consideration of the above assumptions and application of the measured particle data the terminal velocities of the fallout particles were calculated from aerodynamic falling equations. (See Appendix E.) The atmosphere was then divided into 5000-ft increments from the surface to 100,000 ft and the average wind speed and direction within these increments was determined. With knowledge of the rate of fall of the various size particles and the wind vectors acting on these particles their trajectories were computed. Particles of 2000, 1500, 1000, 750, 500, 375, 250, 200, 150, 100, 75, 50, and 25 μ in diameter were placed at 5000-ft increments in the cloud model. Each particle size at each starting elevation was then followed through the atmosphere. Comprehensive use of the available wind data was made in computing the particle trajectories. Effects of both space and time variations on the winds were fully considered. The upper air data from Eniwetok, Bikini,

BUT ENIWETOK WAS 200 MILES WEST OF BIKINI
SO THE WIND PATTERN THERE WAS IRRELEVANT!

[redacted]

and Rongerik Atolls from 0 hr through 0 + 6 hr were used. Since the primary fallout was deposited over the area between Bikini Atoll and Rongelap Atoll within the first 8 hr, no extrapolation of the wind data was necessary for these particles. However no wind data after H + 6 hr were available for the area beyond the Rongerik Atoll and a time extrapolation had to be used in determining the winds that fixed the particle trajectories there. In plotting the trajectories it became obvious that particles above 1000 μ in diameter would fall very near ground zero. Consequently, no calculations were made on the 1000, 1500, and 2000 μ particles.

Figure 6.5 shows the terminal points of the 231 trajectories evaluated. The primary effect of the larger particles is evident at distances close to ground zero.

6.2.5 Consideration of Cloud Dimensions

The maximum lateral width of the fallout area was determined by expanding each particle's arrival point to the diameter of the stem or cloud from which the particle originated. From the cloud photography data the stem diameter was found to be 6.6 miles, the stem height 60,000 ft, the cloud diameter 66 miles and the cloud height 100,000 ft at 0 + 10 min. These dimensions were chosen although the cloud continued to expand laterally after 0 + 10 min. For simplicity it was assumed in this model that the cloud and stem were cylinders having these dimensions. This evaluation assumes no cloud diffusion with time, but fully considers shear.

6.2.6 Determination of Axis of Symmetry of the Fallout Pattern

From the swath of points (Fig. 6.5) the direction of fallout was determined. Since the particle arrival points had a narrow spread it seemed reasonable to construct an axis about which the fallout was symmetrical. Such a symmetrical fallout pattern results only if the upper winds have the necessary configuration for so restricting the particle trajectories. The time of arrival of the particles was also calculated, Table 6.6. Some of the calculated trajectories of the smaller particles starting at high elevations did not reach the surface until many hours after the main body of material had deposited. These arrival points indicative of secondary fallout were not considered in the determination of the axis of symmetry.

6.2.7 Construction of the Fallout Pattern

Using the established axis of symmetry of fallout in conjunction with the measured levels of gamma activity on the available atolls a complete fallout pattern (r/hr at 1 hr) was constructed as presented in Fig. 6.6. This pattern shows the levels of fallout that would exist on an infinite land plane should the basic assumptions used in the definition of the experimental model hold. It is important to note that this pattern was constructed solely on consideration of the gamma field measurements and the axis of symmetry: however, there is other supporting

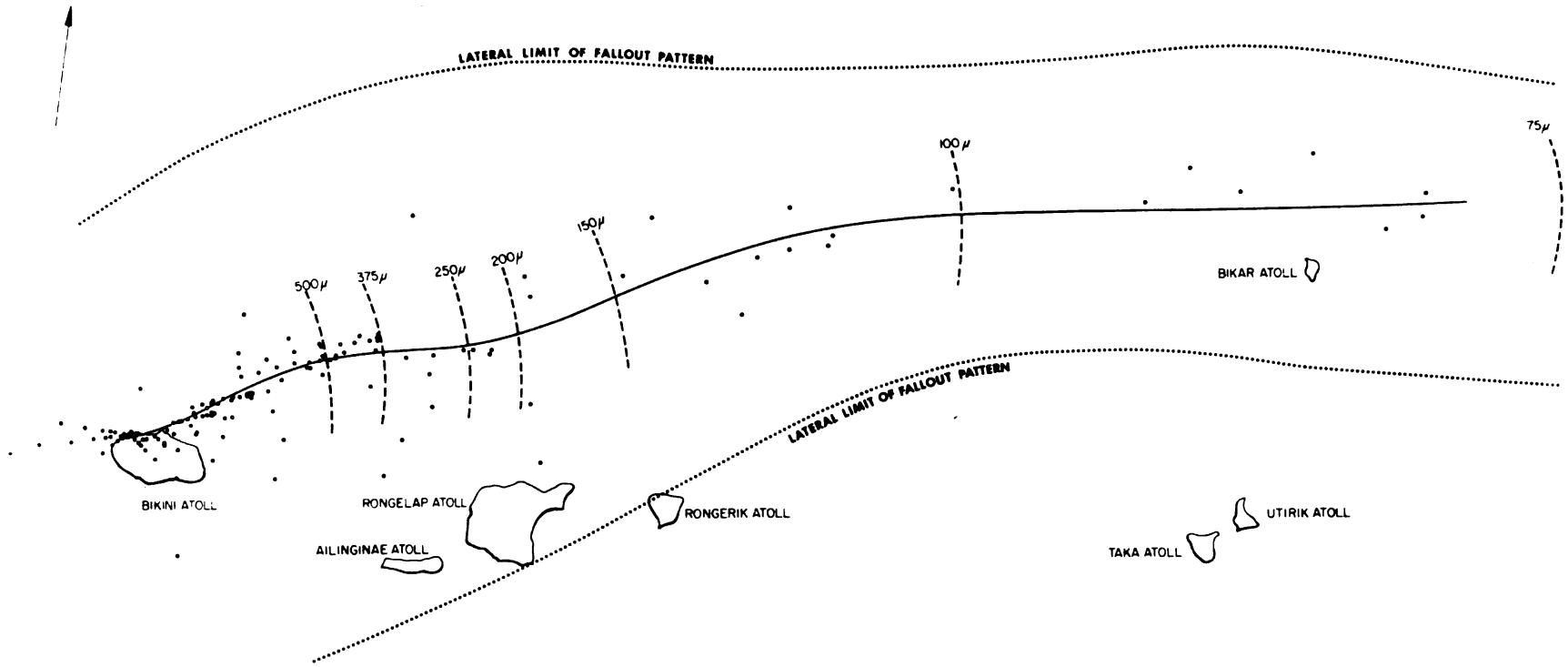

Fig. 6.5 Shot 1, Calculated Direction of Fallout From Analysis of Particle Trajectories (dashed lines indicate limiting distance of stated particle sizes)

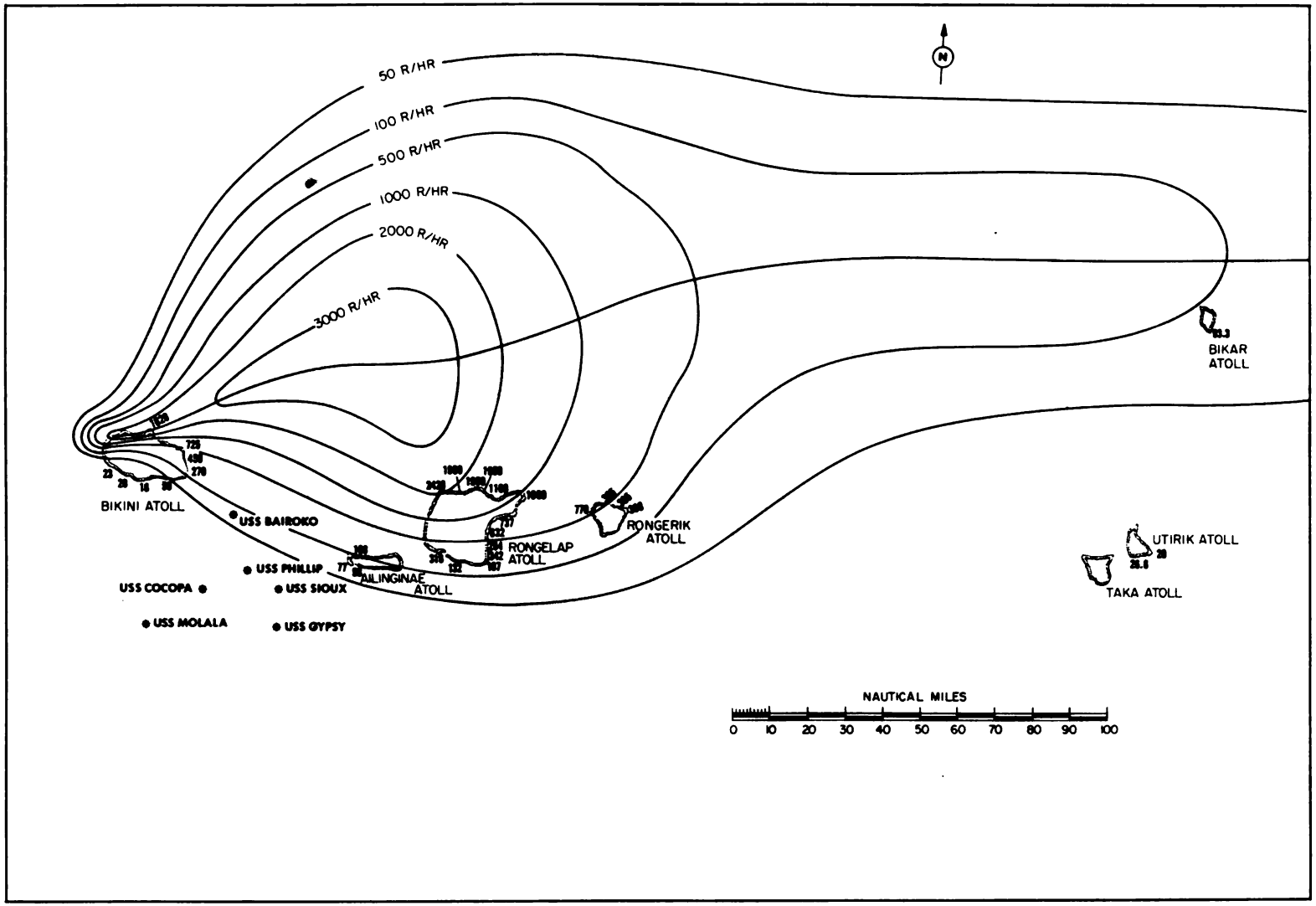

Fig. 6.6 Shot 1, Reconstructed Complete Fallout Pattern (r/hr at 1 hr)

evidence available from the analysis of the particle trajectories. The maximum lateral dimension of the fallout pattern as indicated in Fig.6.5 agrees well with the constructed pattern. The density of arrival points should be related to the levels of activity; this offers further reason to construct the area of peak activity to the north of Rongelap Atoll.

6.2.8 Evaluation of the Shot 1 Fallout Pattern

To determine the time of arrival of fallout, Fig. 6.13 was constructed based on the times as determined from the particle trajectory analysis. Included in the analysis was the effect of the cloud dimensions. Comparison of this calculated time of arrival with the reported time of arrival on the outer islands indicates the validity of the calculated rates of fall of the particles. Table 6.6 presents this comparison.

TABLE 6.6 - Shot 1, Comparison of Calculated and Observed Times of Arrival of Fallout

Distance (n miles)	Calculated Time of Arrival (hr)	Observed Time[a] of Arrival (hr)
14	1.1	1
50	2.1	-
87	4.7	7
100	5.9	-
126	7.8	8
150	8.9	-
200	11.1	-
250	13.2	-
302	15.4	18

(a) Taken from Reference 1.

The reliability of the observed times of arrival on the atolls inhabited by natives are open to some question because of poor documentation. This appears to be especially true of the 7 hr arrival time at the atoll of Rongelap. The weather island of Rongerik at 126 nautical miles reported observed arrival times that compare well with the calculated values.

An attempt to determine the average period of fallout was made by evaluating the trajectory data as shown in Fig. 6.13. This was done by obtaining an average time of cessation of fallout. The rate of arrival of fallout at How Island caused the majority of the activity to be deposited early in the total period of fallout (see Section 5.7). On the basis of this observation the curve indicating the time of cessation of fallout (Fig. 6.13) was weighted showing the period of fallout ending before all particulate had arrived. It is at this time that the level of gamma activity peaks. Continuing fallout after this time is of

[redacted]

such small magnitude that decay is greater than build-up.

Another check on the validity of the analysis using the experimental model was a comparison of the particle size distribution as measured from samples collected on the atolls and the size distribution that would be expected from consideration of the trajectories of the particles. Table 6.7 tabulates the measured particle size distribution found in samples from the atolls as taken from the data presented in Chapter 5.

TABLE 6.7 - Shot 1, Measured Particle Size

Station	Smallest Particle (μ)	Largest Particle (μ)	Geometric Mean (μ)
Bikini	<25	>1000	112
Ailinginae	16	172	60
Rongelap Village	10	126	
Rongelap North End	16	394	70
Rongelap, Kabelle	16	518	
Utirik	6	134	45

The calculated trajectories showed particles from 2000 to 100 μ arrived as primary fallout within the Bikini Lagoon. This fact agrees very well with the measured size distribution shown in Table 6.7. Consideration of the cloud diameter and stem diameter, in the experimental model, on the arrival points of the particle trajectories indicates particles from 150 to 75 μ diameter would arrive at the north end of Rongelap with the limit of the 250 μ particles falling approximately 10 nautical miles north of Rongelap Atoll. The steep gradient of particle size distribution in a north-south line is also clearly indicated from the model study which agrees well with the size distribution found at Ailinginae some 15 nautical miles south of north Rongelap. Also the calculated size limits the particles arriving at a distance or 300 nautical miles to a maximum diameter of 75 μ as compared to a measured geometric mean size of 45 μ.

The only discrepancy of any magnitude between observed data and those calculated from the experimental model is that no fallout arrived at Utirik based on the model analysis. It must be realized that at this distance the model analysis is weakest because the wind data used were extrapolated as being constant from 0 + 6 hr to 0 + 20 hr, the latter being the time of arrival of fallout at a distance of approximately 300 nautical miles. This extrapolation was necessary because no wind data for periods beyond 0 + 6 hr was available at the time of this analysis.

Even better correlation of measured to calculated particle size would be obtained if a larger cloud diameter were used in the experimental model. For this analysis the value used of 66 nautical miles was conservatively chosen; Project 9.1 cloud dimension data indicate

the cloud continued to grow laterally to a diameter larger than 66 nautical miles at the time of their last reported measurement, 0 + 10 min.

The fallout contours from this analysis indicate higher levels of activity 60 nautical miles distant than those existing within 10 miles of the detonation point. The pattern is much wider than would be obtained by scaling the surface shot from Operation JANGLE. For matters of comparison surface JANGLE was scaled to 15 MT by the cube root scaling relationship. This pattern is shown in Fig. 6.7 on the same map scale as the Shot 1 pattern presented in Fig. 6.6. The resulting comparison is interesting, primarily from the point of view of the extreme variation in the configuration of the two patterns. Justification of fallout contours of higher yield devices having little or no relationship to the scaled JANGLE surface detonation contours is evidenced in an analysis of cloud dimensions with respect to yield.[11] The reference indicates that a change of cloud shape takes place with increasing yields becoming gradually flattened for higher yields. This flattening effect would indicate a resulting wider pattern than one would obtain by simply scaling the JANGLE surface data.

This configuration is also evidenced in the analysis of the Shots 5 and 6 fallout patterns.[4]

6.2.9 Material Balance for Shot 1

Two material balances were made on the resulting Shot 1 fallout pattern. The bases for these balances were theoretical in one case and experimental in the other. (See Appendix F.)

The theoretical calculations resulted in 57 per cent of the measured yield of the Shot 1 device being accounted for within the 100 r/hr at 1 hr contour. Also, the theoretically calculated fraction of the device deposited at Station 251.03 was found to be 7.0×10^{-16}/sq cm.

The fallout in a total collector located at Station 251.03 was analyzed radiochemically and the results showed 3.7×10^{-16} of the device was deposited per square centimeter at this location. Extrapolating this ratio over the fallout pattern after taking into consideration the varying levels of activity resulted in approximately 30 per cent of the device being accounted for. This value is questionable because of the fragmentary data upon which it is based. However, the two results indicate that the fallout pattern as constructed for Shot 1 is within reason.

Table 6.8 indicates the average gamma activity in r/hr at 1 hr with respect to the areas over which these fields existed.

TABLE 6.8 - Areas of Average Gamma Activity

Area (sq. miles statute)	Residual Average Gamma Activity (r/hr at 1 hr)
2,040	3,000
2,880	2,500
3,860	1,500
6,030	750
12,900	300

This exaggerates areas of high dose rate contours as compared to dose rate vs. areas for the 1956 Redwing tests, due to inclusion of Eniwetok data from 200 miles West of Bikini in wind pattern, which results in a "hotline" or fallout axis too far North of Rongelap Atoll.

[redacted]

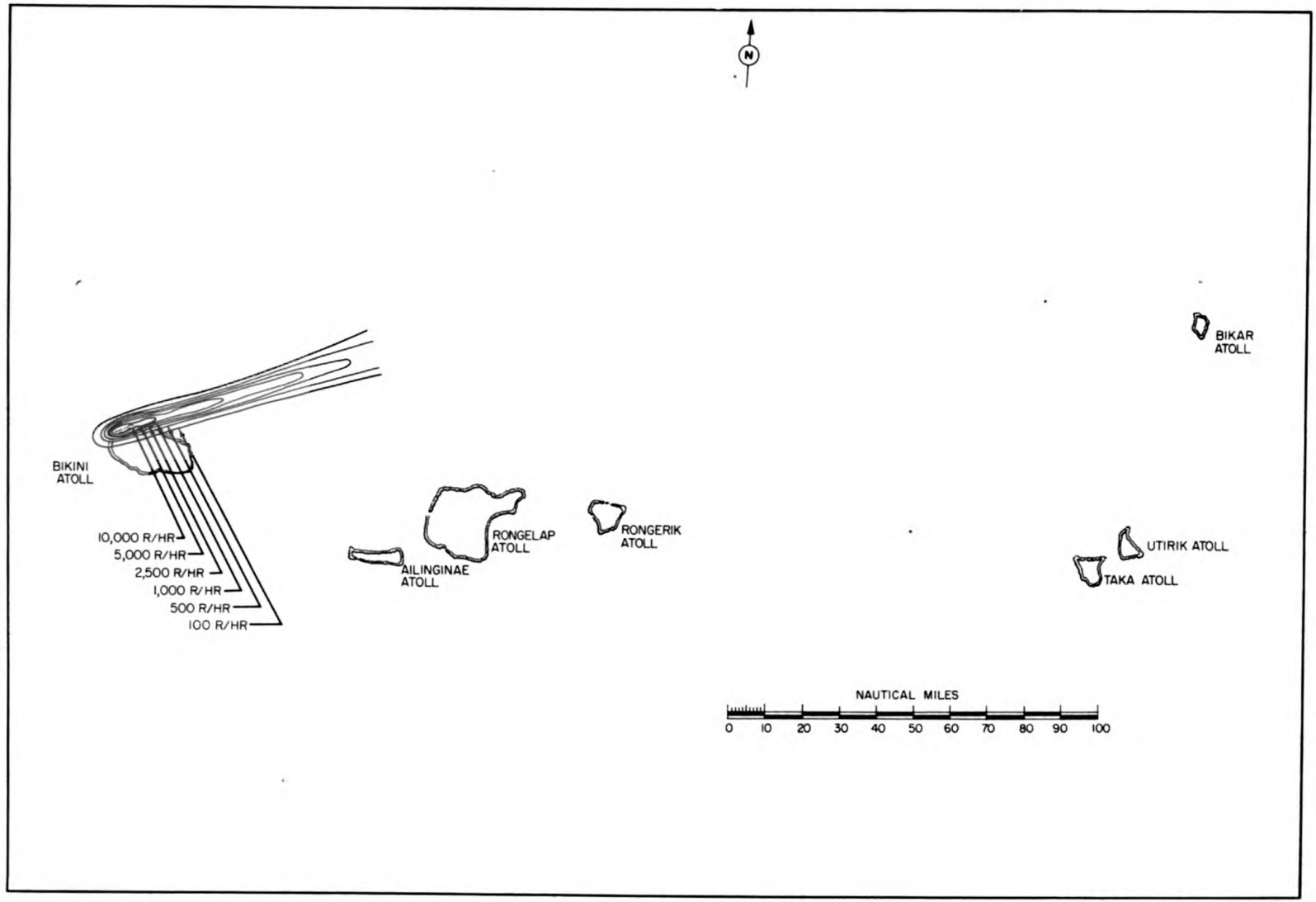

Fig. 6.7 JANGLE Surface Shot Scaled to 15 MT (r/hr at 1 hr)

6.2.10 Growth of Shot 1 Fallout Pattern with Time

It must be realized that the reconstructed fallout pattern described in Fig. 6.6 indicates for convenience the levels of activity t that would exist should all of the fallout particulate be down at 0 + 1 hr. Of course, this is not the case, for the primary pattern out to approximately 280 nautical miles was not static until some 20 hr after shot time. Figures 6.8 through 6.12 show the growth of the pattern with time. The gamma field levels are those that would exist at these times over a land area. In construction of these patterns consideration of both decay and time of arrival as indicated by Fig. 6.13 were taken into account.

6.3 EXTENDED FALLOUT PATTERN FOR SHOT 2

Bikini Atoll was not heavily contaminated after Shot 2 was deton nated due to the primary fallout falling to the north of the shot point. Eleven of the samples from the free-floating sea stations recovered after Shot 2 were evaluated and it was found that the main swath of fallout crossed over the station array. Of the 11 stations recovered seven were in the fallout area as indicated by Table 6.9. The total collector data were reduced and analyzed by Project 2.6a.[18]

TABLE 6.9 - Shot 2, Gamma Infinite Field Levels Converted to r/hr at 1 hr as Determined by Various Techniques

Station	Bearing from Ground Zero (degrees true)	Distance from Ground Zero (n miles)	Gummed Paper Collector Analysis (r/hr)	Total Collector Analysis(a) (r/hr)
A_4	352	43	120	120
O_4	247	34	0.24	2.0
P_4	271	34	1.0	0.1
Q_4	295	34	33	110
R_4	308	36	435	480
T_4	337	43	220	90
A_5	347	52	147	90
D_5	054	53	0	-
E_5	075	53	0	-
F_5	095	53	0	-
G_5	115	53	0	-

(a) As evaluated by Project 2.6a.

[redacted]

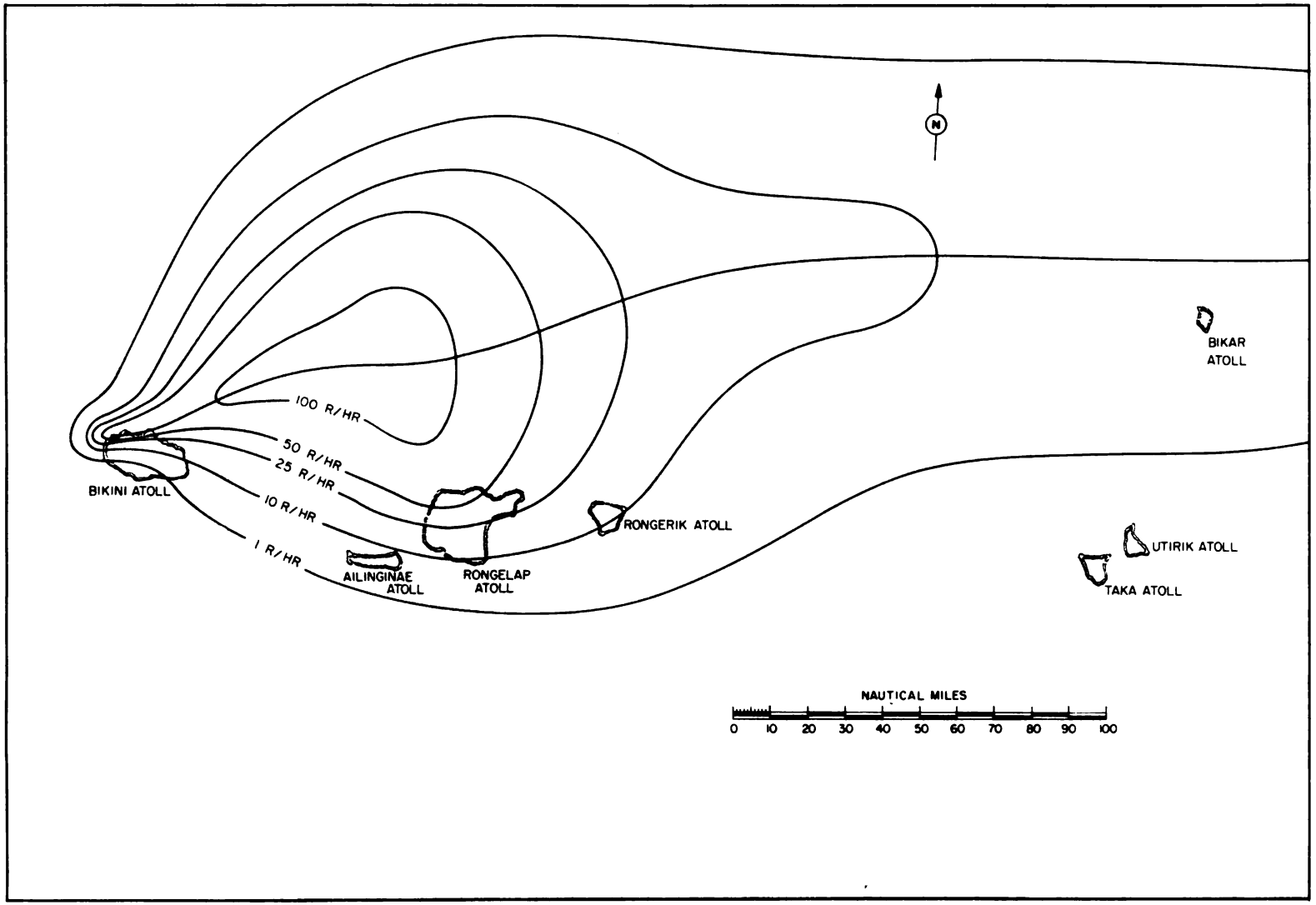

Fig. 6.12 Shot 1, Reconstructed Fallout Pattern at 18 hr

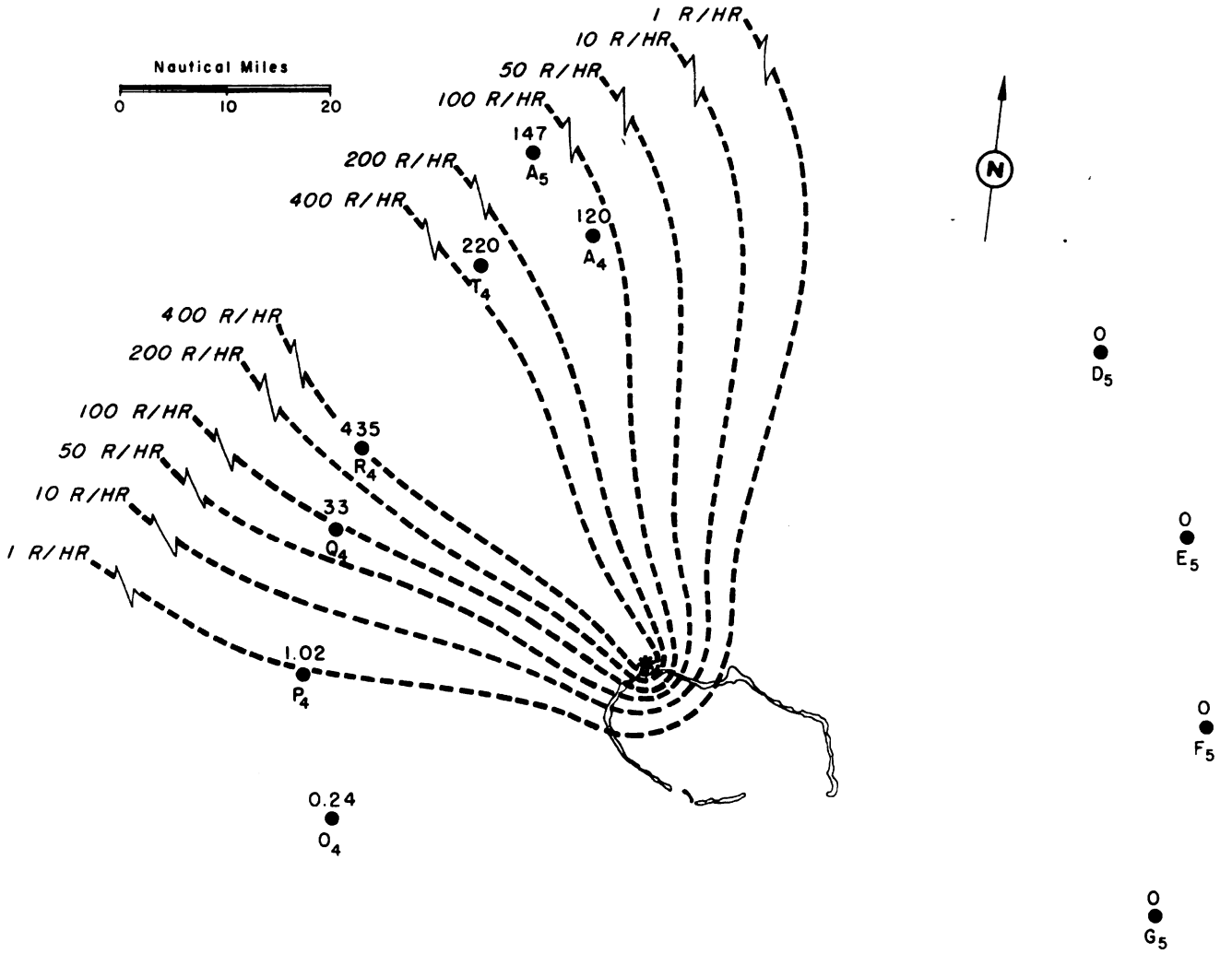

Fig. 6.14 Shot 2, Fallout Pattern (r/hr at 1 hr)

CHAPTER 7

SUMMARY

7.1 GENERAL OBSERVATIONS

The study of thermonuclear explosions at CASTLE has shown the fallout problem to be of considerably greater magnitude than predicted. This demonstration of the radiological capabilities of superweapons makes it imperative that scaling relationships for fallout be derived which will apply over the entire range of possible weapon yields. A common basis of development is required if predictions are to be valid for the now undocumented medium yield range (high yield fission—low yield thermonuclear). Such a basis may be found in the changes in cloud geometry which are known to occur with changes in yield.

The increased coverage by fallout appears to be due to the flattening of the source cloud at high yields in contrast to the more nearly spherical cloud shape of the nuclear model used for the predictions. The following general observations may be drawn concerning fallout from the more diffuse source:

(a) The extent of land gamma radiation fields of military significance is increased beyond that directly attributable to the increase in yield over the nuclear range.

(b) This increase in the area of lethality is the result of a more even distribution of fallout over a larger area. Stating it another way, reduction of the extra-lethal or over-kill factor extends the lethal range for fallout.

(c) The increased efficiency with which superweapons disperse radioactive materials is to some extent counter-acted by the delay in arrival of fallout from the high source cloud and the rapid rate of decay which occurs in the interim.

7.2 PLANS FOR FURTHER WORK

Further study of the interaction of these three factors and comparisons with model data are expected to reveal the part cloud geometry plays in the distribution of fallout. Correlation of data from all CASTLE sources, including the results of water sampling under Project 2.7, will be made using the USNRDL experimental model. Idealized gamma

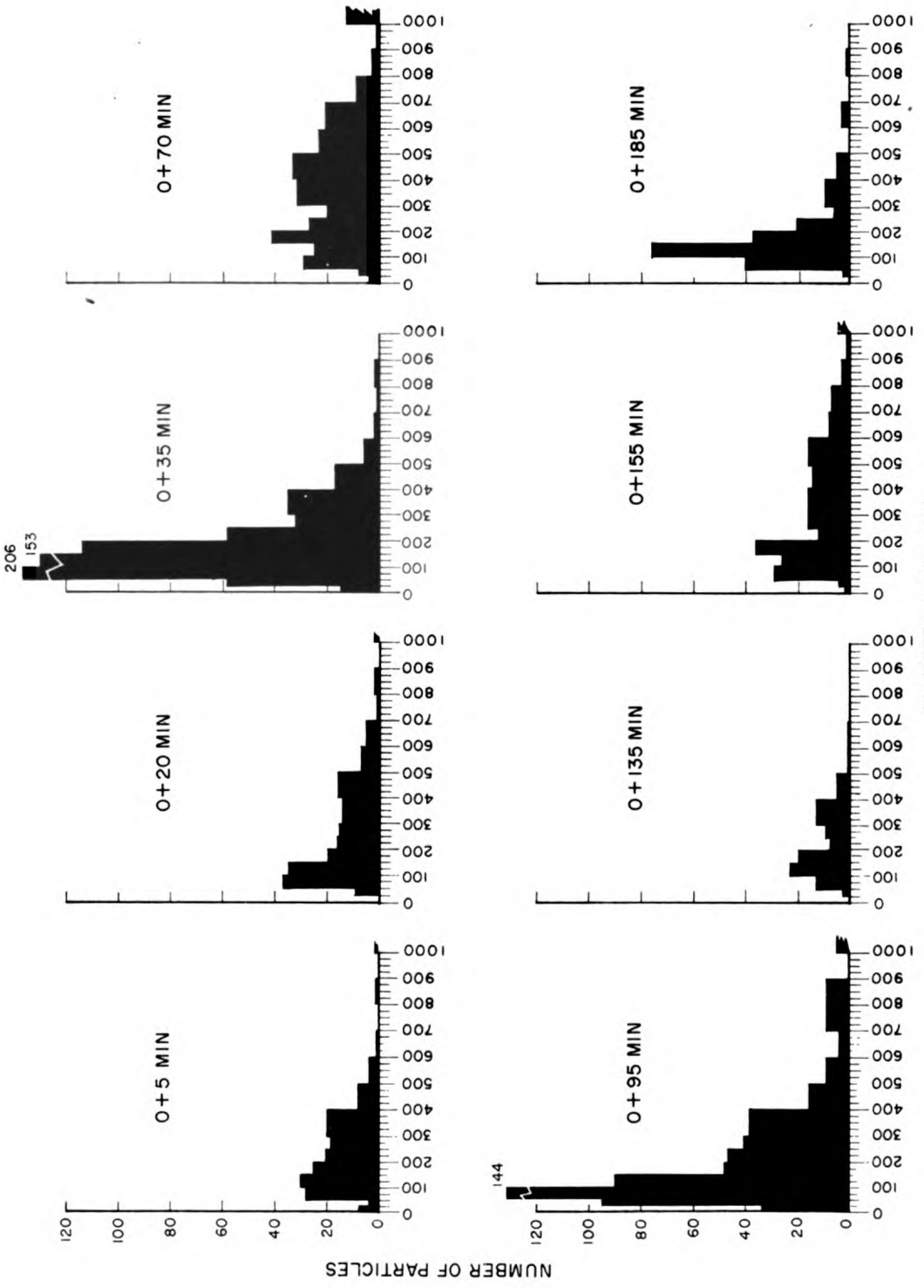

Fig. C.1 Shot 1 Particle Size Distribution, Station 250.04

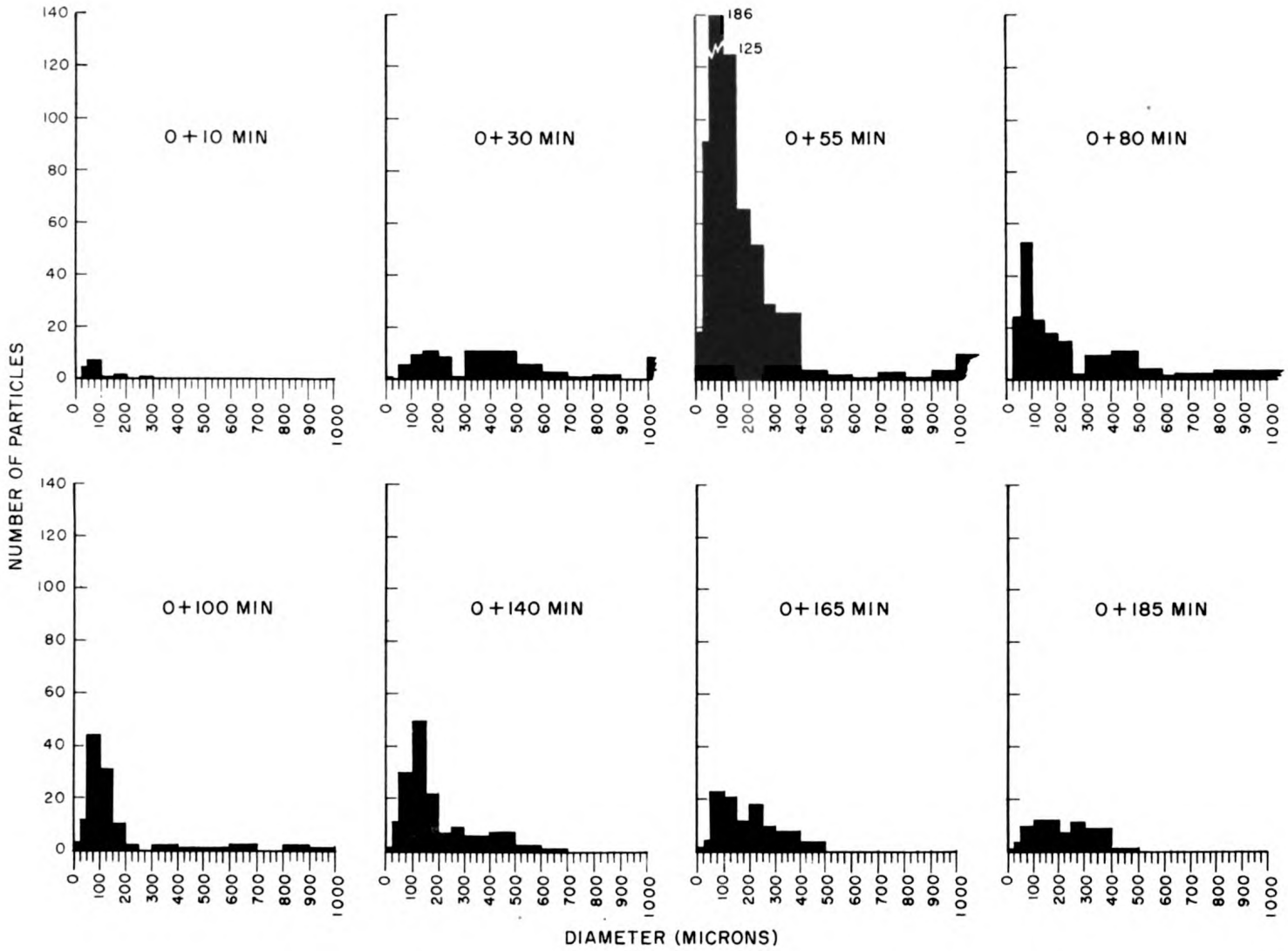

Fig. C.5 Shot 1 Particle Size Distribution, Station 251.04

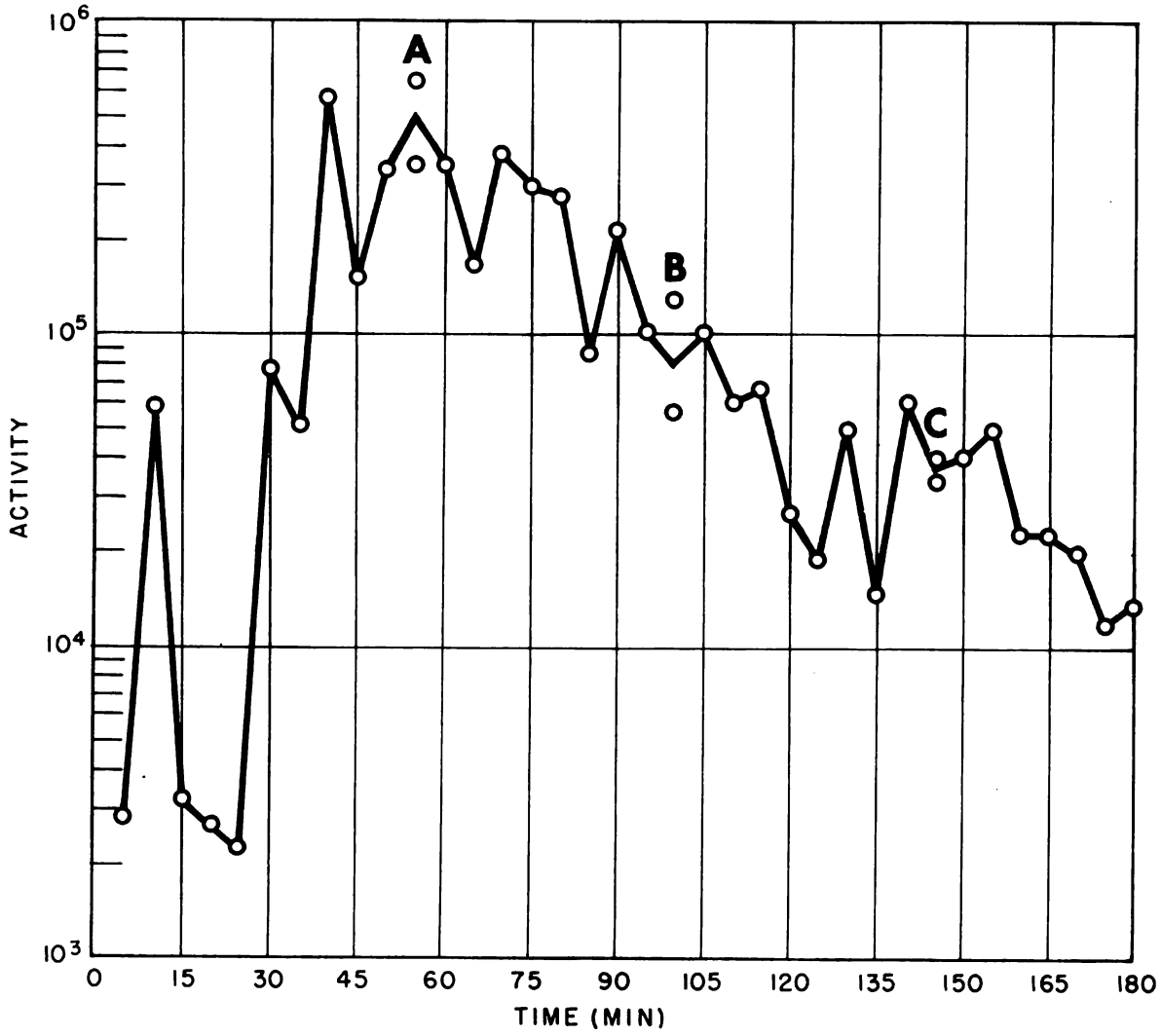

Fig. C.13 Shot 1, Time of Arrival and Period of Fallout, Station 251.04

[redacted]

APPENDIX D

FALLOUT PARTICLE DENSITY, SHOT 1

TABLE D.1 - Differential Fallout Collector 250.04

Sample No.	Sampling Time min after ABD	Density (g/cu cm)	Average Diameter (μ)	γActivity (c/m)	Date Counted	Color
1	25	2.28	1480	53	7/20	white with orange tinge
2	40	2.05	1020	84	7/20	white
3	40	2.54	900	86	7/19	grayish white
4	50	2.24	580	89	7/20	white
5	55	2.22	730	210	7/20	white
6	75	2.42	1060	110	7/19	gray
7	80	2.26	810	230	7/19	white
8	85	2.52	350	21	7/20	white
9	90	2.52	750	47	7/23	white
10	95	2.18	675	502	7/20	white
11	100	2.17	550	66	7/19	white
12	105	2.10	500	40	7/21	white
13	110	2.24	630	0	7/21	white
14	125	2.19	590	105	7/21	white
15	130	2.41	540	64	7/21	white
16	135	2.22	260	19	7/21	white
17	130	1.78	490	13	7/19	white
18	140	2.18	350	44	7/21	white
19	140	2.35	590	84	7/21	white
20	140	2.21	530	231	7/21	white
21	145	2.23	310	34	7/21	white
22	145	2.40	480	36	7/21	white
23	145	2.04	650	106	7/21	white
24	150	2.38	340	61	7/22	white
25	160	2.27	380	64	7/22	white
26	160	1.94	700	99	7/23	white
27	160	2.38	515	62	7/23	white
28	165	1.65	620	66	7/23	white
29	165	2.10	375	2	7/23	white
30	170	2.67	570	13	7/19	white
31	175	2.32	325	44	7/19	white
32	185	2.20	325	24	7/19	white

TABLE D.3 - Differential Fallout Collector 250.24

Sample No.	Sampling Time (min after ABD)	Density (g/cu cm)	Average Diameter (μ)	γ Activity (c/m)	Date Counted	Color
1	5	2.11	420	0	7/22	white
2	10	2.40	980	0	7/22	white
3	15	2.38	425	0	7/22	white
4	20	2.22	240	26	7/22	white
5	25	2.75	275	12	7/22	white
6	35	2.66	675	160	7/22	white
7	50	2.62	1410	146	7/23	white
8	60	2.46	335	0	7/23	white
9	65	2.38	220	0	7/23	white
10	65	2.54	535	33	7/23	white
11	65	2.55	440	42	7/23	white
12	65	2.60	340	43	7/23	white
13	65	2.59	250	65	7/23	white
14	65	2.48	250	44	7/23	white
15	65	2.36	590	141	7/23	white
16	80	2.58	200	7	7/23	white
17	90	2.45	270	31	7/23	white
18	150	2.05	310	24	7/23	white

[redacted]

TABLE E.2 - Tabulated Terminal Velocities of Various Sized Particles Starting at Various Elevations

Altitude (ft)	Terminal Velocity (ft/hr)											
	10 μ	25 μ	50 μ	75 μ	100 μ	150 μ	200 μ	250 μ	375 μ	500 μ	750 μ	1000 μ
Surface	49.3	308	1230	2780	4480	7,375	10,300	13,100	20,400	27,600	42,000	56,500
2,000	55.8	349	1390	3140	4820	7,870	10,900	14,000	21,600	29,300	44,500	59,800
4,000	57.1	357	1430	3210	4950	8,100	11,200	14,400	22,200	30,100	45,800	61,600
6,000	57.2	358	1430	3220	5030	8,250	11,500	14,700	22,700	30,700	46,800	62,900
8,000	57.3	359	1440	3230	5100	8,380	11,700	14,900	23,100	31,300	47,700	64,100
10,000	57.7	361	1440	3250	5210	8,570	11,930	15,300	23,700	32,100	48,930	65,800
12,000	58.3	365	1460	3280	5320	8,760	12,200	15,660	24,300	32,900	50,100	67,300
14,000	59.0	369	1470	3320	5400	8,930	12,500	16,000	24,800	33,600	51,200	68,800
16,000	59.1	370	1480	3330	5520	9,140	12,800	16,400	25,400	34,500	52,500	70,600
18,000	59.6	373	1490	3360	5630	9,340	13,000	16,700	26,000	35,300	53,800	72,300
20,000	60.6	379	1520	3420	5760	9,570	13,400	17,200	26,700	36,200	55,200	74,300
25,000	61.1	382	1530	3440	6000	10,000	14,000	18,000	28,100	38,100	58,100	78,200
30,000	64.1	401	1600	3610	6370	10,700	15,000	19,300	30,000	40,700	62,200	83,700
35,000	67.1	420	1680	3780	6900	11,600	16,200	21,000	32,600	44,400	67,700	91,000
40,000	69.4	434	1730	3910	6940	12,400	17,400	22,500	35,200	48,000	73,400	98,800
45,000	71.4	446	1780	4020	7140	13,200	18,800	24,300	38,100	51,900	79,400	107,000
50,000	74.9	469	1870	4220	7500	14,300	20,300	26,300	41,300	56,400	86,500	117,000
55,000	74.9	469	1870	4220	7500	14,500	20,700	26,900	42,500	58,000	89,200	120,000
60,000	74.9	469	1870	4220	7500	16,200	23,300	30,400	48,300	66,100	102,000	137,000
65,000	74.9	469	1870	4220	7500	16,900	24,800	32,500	51,800	71,200	110,000	148,000
70,000	74.9	469	1870	4220	7500	16,900	26,200	34,600	55,400	76,300	118,000	160,000
75,000	74.9	469	1870	4220	7500	16,900	27,700	36,800	59,300	81,900	127,000	172,000
80,000	74.9	469	1870	4220	7500	16,900	29,000	38,700	62,900	87,100	135,000	184,000
85,000	74.9	469	1870	4220	7500	16,900	30,000	40,800	66,900	93,000	145,000	197,000
90,000	74.9	469	1870	4220	7500	16,900	30,000	43,400	71,700	100,000	157,000	213,000
95,000	74.9	469	1870	4220	7500	16,900	30,000	45,500	75,800	106,000	167,000	228,000
100,000	74.9	469	1870	4220	7500	16,900	30,000	47,700	80,400	113,000	179,000	244,000

APPENDIX F

DETERMINATION OF MATERIAL BALANCE FOR SHOT 1 FALLOUT PATTERN (r/hr at 1 hr)

In determining the material balance for a given fallout pattern, it is necessary to relate the amount of activity accounted for within the fallout contours to that produced in the detonation.

The gamma field surveys of the outer islands were made from 8 to 10 days after Shot 1. The following material balance was calculated for time t = 0 + 9 days. Selection of this time eliminated the introduction of any possible errors due to extrapolation of the field measurements to early times. Furthermore, experimental data on the gamma energy spectrum were available for this time period.

F.1 PER CENT OF DEVICE ACTIVITY AT TIME (t)

Let Y_t = total No. of photons/sec at time (t)

F = fission yield of the device in KT

A = No. of fissions/KT of yield

N_t = d/s/10^4fissions at time (t)

r_t = beta particle to gamma photon ratio at time (t)

then

$$Y_t = \frac{F\,A\,N_t \times 10^{-4}}{r_t} \quad \text{photons/sec}$$

F = 9000 ± 1000 KT

A = 1.5×10^{23}

N_t = 4.93×10^{-3}

r_t = 0.45

Computation of N_t was made for Shot 5 at 0 + 9 days.[4] Consideration was made of the contribution from fission products as well as that from U^{239} and U^{237} induced activities. Since the capture to fission ratio for Shot 1 and Shot 5 were nearly the same these data were assumed reasonably valid for Shot 1 calculations. Similarly the beta particle to gamma photon ratio calculated for Shot 5 at 0 + 9 days was used in this evaluation.[4]

Therefore,

$$Y_t = \frac{(9 \times 10^3)(1.5 \times 10^{23})(4.93 \times 10^{-3})(10^{-4})}{0.45}$$

$$Y_t = 1.47 \times 10^{21} \text{ photons/sec at 0 + 9 days.}$$

F.2 RELATION OF DEPOSITED ACTIVITY TO GAMMA FIELD AT 3 FT FOR AN INFINITE CONTAMINATED PLANE

Let I_t = radiation intensity in r/hr at time (t) 3 ft above an infinite contaminated smooth plane

K = a constant which includes the air absorption coefficient

A_t = deposited activity in μc/sq cm at time (t)

E_t = average gamma source energy in Mev/disintegration at time (t)

then[17],

$$I_t = KA_tE_t.$$

Let B = dose build up factor[6] or the ratio of the dose from all photons to that from unscattered photons

R = source energy degradation caused by roughness of the plane[10]

then,

$$I_t' = (KA_tE_t)(B)(R),$$

where

I_t' = radiation intensity at time (t) in r/hr at 3 ft as measured in the field

or

$$A_t = \frac{I_t'}{K\,E_t\,B\,R}\ \mu c/\text{sq cm};$$

however,

$$\text{photons/sec/sq cm} = \frac{(\mu c/\text{sq cm})(3.7 \times 10^4)}{r_t}$$

and

$$E_t = \frac{E_t'}{r_t}$$

where

E_t' = average gamma energy in Mev/photon.

Therefore,

$$A_t = \frac{(I_t')(3.7 \times 10^4)}{(K)(E_t'/r_t)(B)(R)(r_t)} = \frac{3.7 \times 10^4\, I_t'}{K\,E_t'\,B\,R}\ \text{photons/sec/sq cm.}$$

Let I_t' = 1 r/hr at 0 + 9 days

K = 0.12 (ref 7)

B = 1.45 (ref 6)

R = 0.60 (ref 10)

E_t' = 0.344 Mev/photon at 0 + 8 days.

The value of the average gamma energy was experimentally determined from a Shot 5 sample at 0 + 8 days.[4] The gamma spectrum experienced little change over the period 0 + 8 to 0 + 10 days and its applicability to Shot 1 calculations has been indicated.*

Therefore,

$$A_t = \frac{(3.7 \times 10^4)(1)}{(0.12)(0.344)(1.45)(0.60)}$$

$$A_t = 1.03 \times 10^6 \text{ photons/sec/sq cm at 0 + 9 days}$$

---

* Private communication from C.S.Cook, USNRDL

[redacted]

or

1 r/hr at 0 + 9 days is produced by an infinitely contaminated plane of uniformly deposited activity of 1.03×10^6 photons per sec per sq cm.

F.3 CALCULATION OF MATERIAL BALANCE

The fallout pattern was evaluated out to the 100 r/hr at 1 hr contour by measuring the areas between contours in sq cm and assuming the arithmetical average of the peripheral contours as the average level of activity for the area segment between the contours. There is some indication that the average value of activity between contours is not arithmetical. However, existing field data do not indicate any one continuous function that describes it precisely. Material balance data for Shot 1 are given in Table F.1.

TABLE F.1 - Material Balance, Shot 1

Contours considered in determination of areas (Fig. 6.6) (r/hr at 1 hr)	Average levels between contours at 0 + 9 days (r/hr)	Area (sq cm)	Total rate (photons/sec)
3000 to center of pattern	3.42	5.3×10^{13}	1.87×10^{20}
2000 to 3000	2.85	7.5×10^{13}	2.2×10^{20}
1000 to 2000	1.71	1.0×10^{14}	1.76×10^{20}
500 to 1000	0.86	1.56×10^{14}	1.38×10^{20}
100 to 500	0.342	3.35×10^{14}	1.18×10^{20}

Therefore, within the 100 r/hr at 1 hr contour 8.39×10^{20} photons per sec are accounted for at 0 + 9 days.

$$\frac{8.39 \times 10^{20}}{1.47 \times 10^{21}} = 0.57$$

Thus, 57 per cent of the device activity is accounted for.

F.4 FRACTION OF THE DEVICE COLLECTED IN TOTAL COLLECTOR, STATION 251.03

A radiochemical analysis[18] on the fallout collected at Station 251.03, where the gamma field reading was 1 r/hr at 0 + 9 days, yielded a value of the bomb fraction over a 1 sq ft area to be 1.5×10^{-13}. This

[redacted]

value was obtained from a total collector sample and must be corrected for collector efficiency which at this dose rate was 43 per cent (see Fig. 4.1). Therefore, the experimentally determined bomb fraction per square foot for a gamma field of 1 r/hr at 9 days equals

$$\frac{1.5 \times 10^{-13}}{0.435} = 3.45 \times 10^{-13}/\text{sq ft} = 3.7 \times 10^{-16}/\text{sq cm}.$$

Since 1 r/hr at 9 days is produced by 1.03×10^{6} photons/sec/sq cm and $Y_t = 1.47 \times 10^{21}$ photons/sec/sq cm the calculated fraction of the device at this station is

$$\frac{1.03 \times 10^{6}}{1.47 \times 10^{21}} = 7.0 \times 10^{-16}/\text{sq cm}.$$

[redacted]

BIBLIOGRAPHY

1. Borg, D., Gates, L.D.,et al.
"Radioactive Fall-out Hazards from Surface Bursts of Very High Yield Nuclear Weapons"
AFSWP 507 May 1954 (SECRET RESTRICTED DATA)

2. Brown, P. and Carp, G.
"Gamma Rate vs Time"
CASTLE Project 2.2 Report
WT-913 (SECRET RESTRICTED DATA)

3. Dallevalle, J.M.
"Micromeritics"
Pitman Publishing Corp, New York, 1948

4. Folsom, T.R., and Werner, L.B.
"Distribution of Radioactive Fallout by Survey and Analysis of Contaminated Sea Water"
CASTLE Project 2.7 Report
WT-935 (SECRET RESTRICTED DATA)

5. Fussel, L. Jr.
"Cloud Photography"
CASTLE Project 9.1
WT-933 (SECRET RESTRICTED DATA)

6. Gates, L.D. Jr. and Eisenhauer C.
"Spectral Distribution of Gamma Rays Propagated in Air"
AFSWP 502A January 1954

7. Heidt, W.B. Jr.,LCDR USN, Schuert, E.A., Perkins, W.W., and Stetson, R.L.
"Nature, Intensity and Distribution of Fallout from M Shot Operation IVY"
IVY Project 5.4a Report
WT-615 April 1953 (SECRET RESTRICTED DATA)

8. Humphreys, W.J.
"Physics of the Air"
McGraw-Hill Book Co., Inc.
New York, 1940

9. Kohman, T.P.
"A General Method for Determining Coincidence Corrections for Counting Instruments"
NNES Vol. IV edited by Seaborg, Katz, and Manning
McGraw-Hill Book Co. Inc. New York (1950)

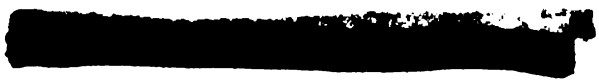

10. Ksanda, C.F.
"Predicted Radiation Levels in Land Target Complexes After Contaminating Atomic Attacks"
U.S. Naval Radiological Defense Laboratory Preliminary Report USNRDL, 15 December 1953 (SECRET)

11. McCampbell, J.M.
"Spheroidal Cloud Theory: A Mathematical Model of Fallout for Nuclear Weapons"
U.S. Naval Radiological Defense Laboratory Technical Memorandum, Technical Memorandum No. 11 September 1954 (SECRET RESTRICTED DATA)

12. Molumphy, G.G.,CAPT USN,and Bigger, M.M.
"Proof Testing of AW Ship Countermeasures"
CASTLE Project 6.4 Report
WT-927 (SECRET)

13 Perry, J.H.
" Chemical Engineers Handbook"
McGraw-Hill Book Co. Inc.
New York, 1941

14 Poppoff , I.G., et al.
"Fall-out Particle Studies"
JANGLE Project 2.5a-2 Report
WT-395 (in WT-371) April 1952 (SECRET)

15 Scoville, H.
"Radiological Survey of Downwind Atolls Contaminated by Bravo"
TU13-54-375,12 March 1954

16. Stetson, R.L., McCampbell, J.M., and Soule, R.R.
"Radiological Capabilities of Nuclear Weapons as Determined by High Explosive Models. I. Shallow Underwater Studies"
U.S. Naval Radiological Defense Laboratory Report
USNRDL-TR-17 October 15, 1954 (CONFIDENTIAL)

17. Teresi, J. and Broido, A.
"Estimation of the Gamma Dose Associated with Radioactive Fallout Material"
U.S. Naval Radiological Defense Laboratory Technical Memorandum, Technical Memorandum No. 18, November 17, 1954

18 Tompkins, E.R., and Werner, L.B.
"Chemical, Physical and Radiochemical Characteristics of the Contaminant at Operation CASTLE"
CASTLE Project 2.6a Report
WT-917 September 1955 (SECRET RESTRICTED DATA)